THE PENNSYLVANIA STATE UNIVERSITY
SCHREYER HONORS COLLEGE

DEPARTMENT OF CIVIL AND ENVIRONMENTAL ENGINEERING

# AN ANALYSIS OF THE BEHAVIOR OF A COMPOSITE STEEL-CONCRETE BEAM

DAVID LEAF
Spring 2012

A thesis
submitted in partial fulfillment
of the requirements
for a baccalaureate degree
in Civil Engineering
with honors in Civil Engineering

Reviewed and approved* by the following:

Dr. Jeffrey Laman
Professor of Civil Engineering
Thesis Supervisor

Dr. Patrick M. Reed
Associate Professor of Civil Engineering
Honors Adviser

* Signatures are on file in the Schreyer Honors College.

## ABSTRACT

Composite steel-concrete beams are common structural members. Among the many applications, composite beams are typically used in floor systems. The Pennsylvania State University conducts composite beam test demonstrations for educational purposes. In the demonstrations, a composite beam is subjected to flexure only. Before each test, the ultimate strength of the composite beam is predicted using the design specifications provided by the American Institute of Steel Construction. During the test, the composite beam has been observed to fail before it reaches its predicted strength. Longitudinal cracking of the concrete slab and interlayer slip have also been observed. These observations have been consistently made. Several complete sets of data have been maintained from these tests. This paper analyzes the ultimate strength of the composite beam using currently available methods. Partial composite action is considered. Additionally, finite element models of the composite beam were developed and analyzed using SAP2000. The analyses are compared to the data obtained from the test demonstrations. Based on the results of these analyses, recommendations for design considerations have been made which will allow the full strength of a composite beam to be achieved.

# TABLE OF CONTENTS

# LIST OF FIGURES

# LIST OF TABLES

# Chapter 1 Introduction

## 1.1 Background

The typical floor system in a building utilizes a concrete slab. Steel beams are commonly used to support the slab. Most often, the steel beams are joined with the concrete slab so the two materials can work together as a series of composite beams. The use of composite beams allows smaller steel shapes to be used, and smaller static deflections to be experienced, which result in a more economical design.

The most common composite beam consists of a W shape steel beam and a concrete slab connected using steel anchors. Typical cross sections of this type of composite beam are shown in Figure 1-1. The type of steel anchor that is most frequently used is a headed shear stud, as seen in Figure 1-2. Steel anchors are welded to the steel beam and encased in the concrete. The anchors transfer the shear forces between the steel and concrete so the two materials can act together as one member.

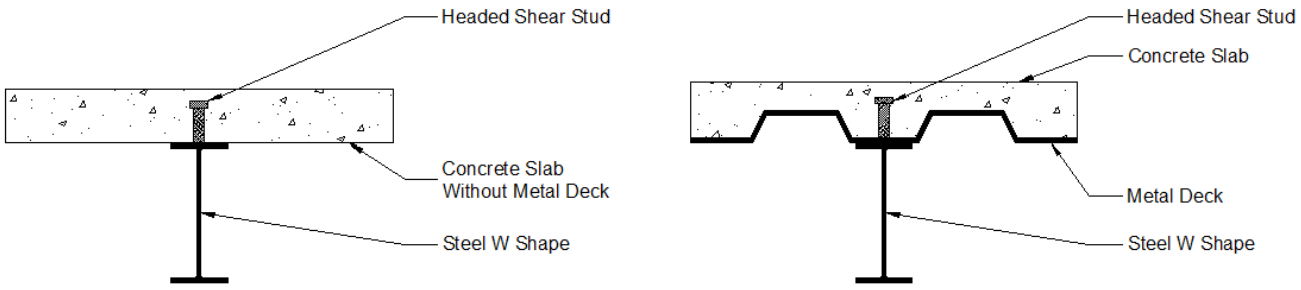


Figure 1-1 Typical Composite Beam Cross Sections

Figure 1-2 Headed Shear Stud

The American Institute of Steel Construction (AISC) provides the design and construction specifications in Chapter I of the AISC manual. If the shear connection is capable of transferring all of the forces between the two materials at the point when one of the materials reaches its full capacity, the connection is considered to be rigid, and the member is considered to have full composite action. If the connection is not capable of transferring all of these forces, the beam only experiences partial composite action. In this case, the connection allows for the materials to move in relation to each other. This is known as interlayer slip. In either case, the shear connection is very influential on the behavior of a composite beam (Geschwindner 2008).

**1.2 Problem Statement**

At the Pennsylvania State University, a demonstration of a composite beam is provided for civil engineering students each year. The composite beam consists of a steel, W10x17, beam and a concrete slab that is loaded with a concentrated load at midspan. The beam was designed to meet the provisions of AISC chapter I for a fully composite beam. In these demonstrations, the actual strength of the beam was observed to be lower than the

strength predicted in accordance with AISC. Over the past several years, ten complete sets of data from this demonstration have been recorded. In these ten demonstrations, the predicted strength was overestimated as compared to tests by an average of 6.6%.

There have been several interesting observations made possible by the tests. The tendency for a longitudinal crack to develop along the center of the concrete slab was observed, as shown in Figure 1-3. In many cases the crack was continuous and propagated almost the entire length of the beam. In other cases the longitudinal cracks were not continuous, and developed above the shear studs only.

Figure 1-3 Observed Longitudinal Cracking

Another interesting observation was the occurrence of interlayer slip. This was recognized with the use of a reference line, drawn continuously from the steel onto the concrete slab, perpendicular to the axis of the beam. A discontinuity in the reference line at the interface between the steel and concrete was observed during the tests, which signifies interlayer slip.

The consistent overestimation of strength reveals that the current practice for determining composite beam strength is inaccurate. The presence of interlayer slip indicates that the beam experiences partial composite action and assuming full composite action is incorrect. These observations made during the tests indicate that the method of determining composite beam strength given by AISC is not accurate and some assumptions made are incorrect.

The observations show that there is a need to be able to more accurately predict the strength of a composite steel beam and concrete slab. This entails a better understanding of the interaction between the two materials and the behavior of the shear connection.

### 1.3 Objectives

The main objective of this study is to better understand and predict the behavior of a composite beam. Specific objectives are listed below:

- To evaluate the effect of longitudinal cracking on the behavior of a composite beam
- To better understand the degree of interaction between steel and concrete in a composite beam with headed shear studs.
- To develop a simple method of approximating the strength of a composite beam

## 1.4 Scope

This study is based on the data obtained from The Pennsylvania State University test demonstrations. All tests were conducted on a composite beam with an A992 Grade 50 W10x17 combined with a solid concrete slab connected with a single row of headed shear studs. This study does not include the effects of a concrete slab with metal decking or a connection with any other types of steel anchors.

## 1.5 Tasks

The tasks completed in this study are as follows:

- Review current literature related to the strength of composite members including theoretical solutions, approximate calculation methods, and finite element modeling.
- Overview current methods of composite strength calculation and analyze all data using the provisions of AISC Chapter I.
- Develop a finite element model of the composite beam tested that incorporates the observations made during these tests.
- Develop a simple method to predict the ultimate strength of a composite beam based on the analysis of the recorded data and the results of the finite element model.

# Chapter 2 Literature Review

In this chapter, relevant available literature on composite beams is reviewed and discussed. From this review, it is shown that the behavior of a composite beam depends on the behavior of the connection of the steel beam to the concrete slab. Along with theories to explain the behavior of the connection there are complex methods of exact analysis, simplified methods of approximate analysis, and methods that use finite element analysis. The review of many of the available theories and methods is presented below.

## 2.1 Tests and Theory

Naithani and Gupta (1988) tested three composite steel-beam-concrete-slab combinations to compare the ultimate strength to strength predictions. Three different beams were used to test the effects of the type of shear connection, and the placement of the transverse reinforcement. The first beam tested was configured with a single shear stud at each section with transverse reinforcement equidistant from the studs. This beam failed by crushing of the concrete accompanied by a longitudinal crack, just as observed in the testing demonstrations. The ultimate strength of the beam exceeded the theoretical strength by 8%. Naithani and Gupta tested a second composite beam with the transverse reinforcement located adjacent to the shear studs. In this case, a longitudinal crack was not observed. The ultimate strength of the second beam was 4% higher than the theoretical prediction. The third specimen used two smaller diameter shear studs at each section in place of the larger, single studs. The flexural capacity of this beam was tested to be much larger than the beams with single shear studs. The ultimate strength of this beam was observed to be 45% higher than

expected (Naithani, Gupta 1988). From these tests, it is shown that the shear connection has a significant effect on the ultimate strength of a composite beam.

In composite beams, longitudinal shear forces at the interface caused by bending stress are evaluated for design. Ramm and Jenisch (1997) recognized that additional transverse bending in the concrete slab affects strength of the composite beam. Full scale beam tests, as well as push out tests, were performed to study the effect of transverse bending on composite beams. It was observed that negative transverse bending moments reduced the ductility of the composite beams. In terms of strength, it was found that the effect of transverse bending depended on the magnitude. Large transverse bending moments actually caused an increase in strength of composite beams due to the increase in compression stress at the connection. With large transverse bending moments, longitudinal cracks are kept to a minimum by the transverse reinforcement. In the case with relatively small transverse bending moments, wide longitudinal cracks develop due to having less transverse reinforcement. The compression at the shear connection is not significant enough to make up for these cracks, leading to a decrease in strength. These tests show that longitudinal cracks and transverse bending moments have a significant impact on the load bearing capacity of the slab in a composite beam (Ramm, Jenisch 1997).

Leon and Viest (1997) state that complete interaction cannot be achieved. They provide a qualitative review of many elastic and inelastic theories based on incomplete interaction. Some common assumptions found in inelastic theories include no friction or bond at the interface, no uplift, and that strain distributions are linear. A review of finite element models was also provided. Some finite element models were found to be quite accurate. However, as the authors of this paper point out, these models are most often used

for academic purposes and are for special cases. With current theories reviewed, it was suggested by the authors that there are two areas in need of further development. These are 1) developing a refined model of the shear connection; and 2) simplifying current finite element models (Leon, Viest 1997).

Sapountzakis and Katsikadelis (2003) presented an analog equation method as a solution to the case where deformable shear studs are used. The method neglects uplift, but considers the in-plane shear forces and deformation of the slab and the axial forces and deflection of the steel beam. A computer program was developed to implement this method of calculation. Examples were evaluated and the results were provided graphically. It is known that the shear forces at the interface are reduced as the height of the web of the steel beam is increased. For this analysis, the stiffness of the connection is based on the height of the web of the steel beam. The results show that as the stiffness of the connection decreases, the interface slip increases, the shear forces at the interface decrease, and the lateral deflections of the beam increase (Sapountzakis, Katsikadelis 2003).

Shangahi University (2005) provides an analysis of the strain difference between the steel and concrete in a composite beam. The calculations use partial interaction and the theory of elasticity. The method analyzes a differential element to solve for the strain difference taking slip and curvature into account. The strain difference affects the displacement and load capacity of a beam. The methods of full interaction and partial interaction are compared. In one specific case, the calculated deflection difference was almost 11% between beams considered with partial interaction and full interaction. It is suggested that the full interaction theory should not be used for beam design (Liu, Liu, Zhang 2005).

Girhammar et al. (1993) proposed a complex analysis of composite beam-columns with partial interaction to find internal actions and displacements. Girhammar et al. provide both a first-order and second-order analysis of a sixth-order ordinary differential equation to give what they call an “exact analysis” which allows for interlayer slip. Solutions and examples are given for a simply supported beam with a uniformly distributed load and axial force. Special cases, including full composite action, were also evaluated. In the case of full composite action, slip is set equal to zero, and the connection stiffness tends to infinity. However, as observed in the testing demonstrations, slip still occurs when full composite action is assumed.

Girhammar et al. (2007) again proposed a static analysis of a composite beam or beam-column with partial interaction which accounts for interlayer slip. A differential equation with first and second order solutions is still used. In this proposal, more accurate boundary conditions are used. With these boundary conditions, revised solutions for the internal actions are given. For beam-columns, the buckling load is based on the effective bending stiffness of the partially composite beam. This approach for determination of critical buckling load using an effective bending stiffness is the same as used by Girhammar et al. (1993) with changes to the buckling length coefficients. The methods of exact analysis presented by Girhammar et al. (2007) are in great depth, which causes them to be extremely long and difficult.

## 2.2 Approximate Calculation Methods

After the proposed methods of exact analysis, Girhammar et al. (2009) provided a simpler version. The simplified method allows the use of the effective bending stiffness that

was previously used for buckling to be used for evaluation of flexure. This analysis uses a differential element to define equations for moment, section shear, interface shear, deflection, and axial force for a fully composite member. For approximation of these terms for a partially composite beam, the bending stiffness for the full composite member is replaced with the effective bending stiffness for the partially composite member. The effective bending stiffness for a partially composite beam that is simply supported is defined as

$$EI_{eff} = \left[1 + \frac{EI_\infty/EI_0 - 1}{1+(\mu/\pi)^2\,(\alpha/L)^2}\right]^{-1} EI_\infty \qquad (2.1)$$

where,

$$\alpha L = \sqrt{\frac{Kr^2}{EI_0(1-EI_0/EI_\infty)}}\,L$$

$EI_\infty$= bending stiffness of the fully composite section

$EI_0$= bending stiffness of the non-composite section

$K$ = shear connection stiffness

$r$ = distance between the two centroids

$L$ = length of composite beam

$\mu$ = buckling length coefficient (for a simply supported beam, $\mu$ = 1)

This method is much simpler than the previously proposed methods by Girhammar et al. However, the authors assert that this simplified method is for approximation only and is not suitable for design purposes.

Fabbrocino et al. (1998) also proposed an analysis of composite beams subjected to flexure. The results show that the actual behavior of a composite beam is different from what

is predicted when full interaction is assumed. The method of analysis is based on the understanding that the behavior of composite beams is dependent on the slip distribution and the resulting forces at the interface. In equation 2.2, the slip (*s*) is related to the rotation of the beam (φ) and displacement of the centroids of the two sections (*w*):

$$s = w_s - w_c + \varphi\, d \tag{2.2}$$

where $w_s$ is the displacement of the centroid of the steel, $w_c$ is the displacement of the centroid of the concrete, and d is the distance between the centroids.

By defining this relationship, the derivative of the slip *ds/dz* is shown in equation 2.3 to be a function of the curvature (χ) and strains at the centroids of the two sections.

$$ds/dz = \mathcal{E}_s - \mathcal{E}_c + \chi\, d \tag{2.3}$$

The curvature depends on the interaction force in the beam. For a given curvature, the moment depends on *ds/dz*. The connectedness of the relationships causes the solution to be very difficult and non-linear. An iterative approach using these relationships is proposed, and a general family of moment-curvature relationship curves is provided. The proposed solution is compared to experimental data. The ultimate load prediction came within 1% of experimental results. However, the slip was overestimated by almost 16%. The iterative approach used is oppressive, and it becomes more difficult to converge for beams that are typically considered to act with full interaction (Fabbrocino et al. 1998).

Qiongxi Lui (2011) proposes a new calculation method for the ultimate load of a composite beam. The analysis accounts for the effect of reduced flexural rigidity due to cracking of the concrete. The slip strain is found based on the new flexural rigidity. The slip is found by integrating the slip strain. Since the slip is greatest at the ends of the beams, the

slip at the end is compared to the strength of the shear connectors. From here, the ultimate load of the beam is obtained. For the case of a simply supported composite beam with a concentrated load at mid-span, the equation for maximum load the shear connection can handle when no cracks are present is shown below:

$$P_{u1} = \frac{4S_u + Q_{sh} n k_2 L}{\frac{L^2}{4} k_1} \tag{2.4}$$

where,

$S_u$ = end slip

$Q_{sh}$ = yield strength of studs

$n$ = number of shear connectors between end of beam and L/2

$k_2 = \frac{(h_d+h_b)^2}{(EI)_d+(EI)_b} + \frac{1}{(EA)_d} + \frac{1}{(EA)_b}$

$h$ = distance from centroid of element to interface

Subscript $d$ = property of ductile element (steel)

Subscript $b$ = property of brittle element (concrete)

$L$ = length of beam

$k_1 = \frac{(h_d+h_b)}{(EI)_d+(EI)_b}$

The equation for maximum concentrated load when there are cracks in the concrete over the entire length of the beam is given as:

$$P_{u2} = \frac{4S_u + Q_{sh} n k_2' L}{\frac{L^2}{4} k_1'} \tag{2.5}$$

where,

$$k_1' = \frac{(h_b+h_d)}{(EI)_d+\alpha(EI)_b}$$

$$\mathrm{k}_2' = \frac{(h_d+h_b)^2}{(EI)_d+\alpha(EI)_b} + \frac{1}{(EA)_d} + \frac{1}{(EA)_b}$$

$$\alpha = \frac{2+2\Psi-\Psi^2}{\Psi^3+2\Psi^2+6\Psi+4}$$

$$\Psi = \frac{(EI)_b}{(EI)_d}$$

The calculation method proposed is relatively simple, but it is still a long process. Also, Lui does not compare the results to experimental data (Lui 2011).

Other researchers have provided calculation methods involving longitudinal shear stresses in the composite beam. Segura (1990) proposed a method for evaluating the shear stresses at the interface of the steel and concrete. Gara, Ranzi, and Leoni (2010) proposed a method of evaluation based on the effects of shear lag. Along with others, these methods are long and complex, and are not practical for design.

**2.3 Modeling**

Mirza and Uy (2008) describe the effect of strain profiles on the connection of a composite beam. Since shear studs are subjected to both flexure and shear, they find it is important to evaluate the effect of both. Since the application of both moment and shear causes nonlinearity, ABAQUS was used to create a three dimensional solid element model of the shear studs. The concrete and steel sections were modeled using eight node elements. The shear stud was modeled using a thirty node element. The metal decking was modeled using four node elements, and a two node element was used for the reinforcement. Due to symmetry, only half of a section was used. A push test analysis was run to determine the strength of the shear studs. This model was evaluated using different strain regimes in the

concrete to account for the effects of shear and bending. These different strain distributions can be seen in Figure 2-1.

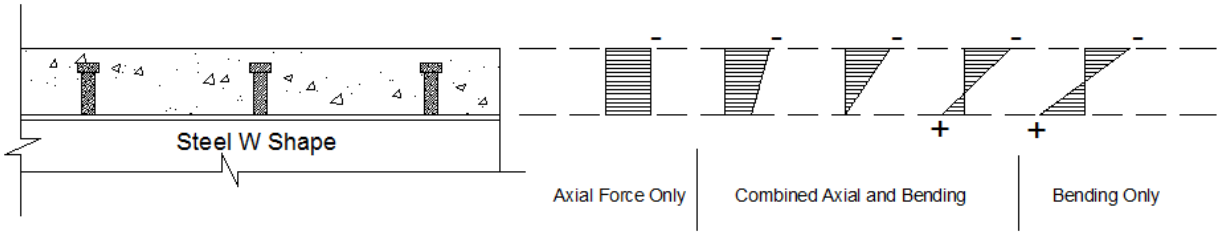


Figure 2-1 Varying Strain Regimes for Push Tests (Mirza, Uy 2008)

The finite element model predicted the strength of the shear studs within 0.7% of experimental data. This shows that the model provides accurate results. With this model, it was found that strain regimes in the solid concrete slab did not significantly affect the strength of the shear stud. This approach provided accuracy only when solid slabs were used (Mirza, Uy 2008).

Ranzi and Zona (2011) compared three different composite beam models. The models are based on the work of Newmark, who used a uniform deformable shear connection to link a concrete slab and steel beam together as shown in Figure 2-2.

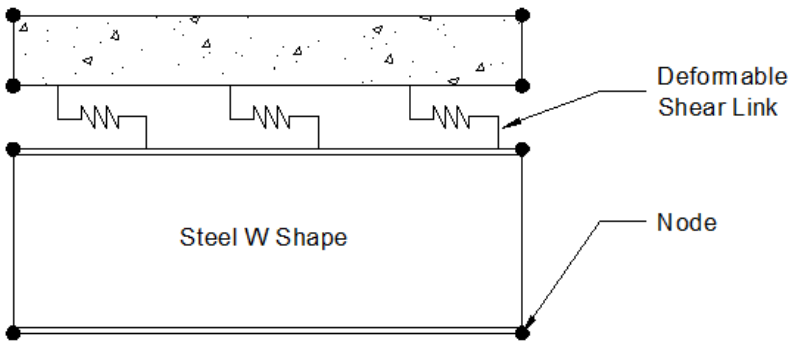


Figure 2-2 Finite Element Model with Deformable Shear Link (Ranzi, Zona 2011)

Newmark modeled the steel beam and concrete slab as two Euler-Bernoulli beams (Ranzi, Zona 2011). Ranzi and Zona (2011) evaluated the model shown in Figure 2 using two Euler-Bernoulli beams, a combination of an Euler-Bernoulli beam (concrete) and a Timoshenko beam (steel), and two Timoshenko beams. The elements were given 10, 13, and 16 degrees of freedom respectively. For the connection, the nonlinear empirical function presented by Ollgaard et al. in 1971 was used (Ranzi, Zona 2011). The models were tested under several loading conditions, and the results were compared to experimental data. For a simply supported beam with a concentrated load at midspan, it was determined that all three models predicted the ultimate load within 2%. For beams controlled by shear, none of the three models provided accurate results. For these beams however, the models using a Timoshenko beam provided much closer failure load predictions than the model using two Euler-Bernoulli beams (Ranzi, Zona 2011).

Earlier work by Ranzi and Zona (2007) provided a much more detailed analysis of the model using an Euler-Bernoulli beam for the concrete and a Timoshenko beam for the steel to include shear deformation. A complex analytical solution was formed using the virtual work principle. This model was evaluated using finite element analysis. Comparing this model to the Newmark model, it was found that the shear deformation of the steel caused more significant effects as the stiffness of the connection increased. Still, for a simply supported beam, these effects were minimal. This model is most relevant for continuous beams and for time dependent analysis (Ranzi, Zona 2007).

He, Li, and Shang (2011) used an element between the steel beam and concrete slab to represent the shear connection in a composite beam. The element was inserted at the interface with a thickness equal to zero. The element was assigned a stiffness to model the

average effect of the shear connectors along the beam. A conceptual image of this type of model is shown in Figure 2-3.

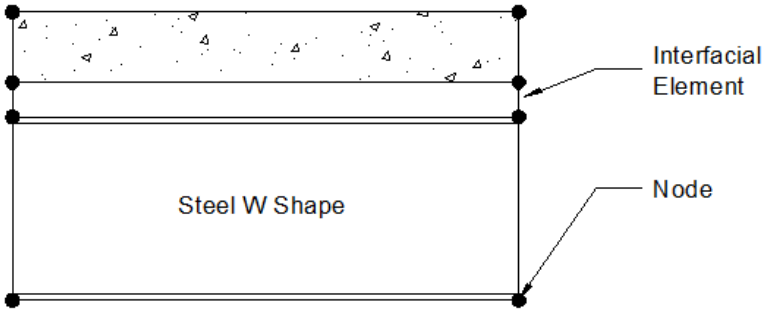


Figure 2-3 Interfacial Element with Zero Thickness (He, Li, Shang 2011)

The results of this finite element model were compared to two different experimental tests. The ultimate load prediction by the model was an overestimation by 5.5% in one test, and 3.5% in the other (He, Li, Shang 2011).

da Silva and Sousa (2009) presented a family of interface elements to account for interlayer slip in a composite beam. Euler-Bernoulli and Timoshenko beam theories were used. Vertical, horizontal, and rotational displacement fields were considered. Various degrees of freedom were used in the different elements. In some elements, shear strain is considered. It was found through a comparison to analytical solutions, that a Timoshenko interface element with quadratic displacement which also accounts for shear strain is the most reliable to use (da Silva and Sousa 2009). Although fairly accurate results are produced, these results cannot be obtained without modeling the beam of interest.

# Chapter 3 Current Methods of Analysis

In this chapter, current methods of analysis using AISC are overviewed. Full composite action and partial composite action are discussed. The composite beam geometry used in the experiments is analyzed using the current methods provided by AISC. The ultimate strengths of the beams tested are calculated in accordance with AISC. In addition, an analysis of the tested beams using the theory of partial interaction is provided.

## 3.1 General

With the use of any method of calculating the strength of a composite beam, the first step is to determine how much of the concrete slab will participate with the steel beam and provide composite action. This is done by finding the effective concrete slab width, $b_{eff}$. The total effective width is found by summing the effective widths for each side of the centerline of the steel beam. According to AISC I3.1a, the effective width for each side is the lesser of the following:

1. 1/8 of the beam span
2. 1/2 of the beam spacing
3. Distance to the edge of the concrete slab

For full and partial interaction between a concrete slab and a rolled W shape, the plastic stress distribution method is used to determine the strength of the section of a composite beam with a compact web. As given by AISC Section I3.2a, The web is considered compact if

$$\frac{h}{t_w} \leq 3.76\sqrt{E/F_y} \tag{3.1}$$

where $\frac{h}{t_w}$ is the web slenderness ratio tabulated in the AISC Steel Construction Manual Table 1-1, E is the modulus of elasticity of steel, and $F_y$ is the yield stress of the steel. If the web is not compact, an elastic analysis of stresses is to be used.

There are two types of interaction between the steel and concrete in a composite beam. These are full composite action and partial composite action. The difference can be depicted with elastic stress distributions, shown in Figure 3-1. For every case, the forces in the concrete and steel are obtained by setting the tensile forces equal to the compressive forces to maintain equilibrium (Geschwindner 2008).

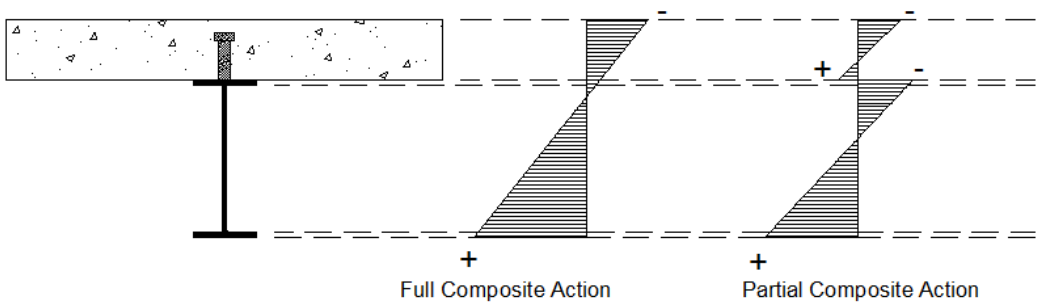


Figure 3-1 Stress Distributions in a Composite Beam (Geschwindner 2008)

### 3.2 Full Interaction

When full interaction is achieved, the shear connection is capable of transferring all forces between the steel and concrete. With full interaction, the shear force between the concrete slab and steel beam,$V'$, is limited by the concrete crushing, or the steel yielding. Determined in accordance with AISC I3.2d, the value is the lesser of the following with consideration of the limit states of concrete crushing or the steel yielding respectively:

$$V_c' = 0.85 f_c' b_{eff} t_s \tag{3.2}$$

or,

$$V_s' = A_s F_y \tag{3.3}$$

where,

$f_c'$ = Compressive strength of concrete

$t_s$ = Concrete slab thickness

$A_s$= Area of steel

If the section is controlled by the steel yielding, $V_c' > V_s'$, and the plastic neutral axis (PNA) is in the concrete slab. The tension in the steel reaches the full plastic capacity and all of the compression is within the concrete slab. The magnitude of the compressive force in the concrete, $C_c$, is equal to the of the capacity of the steel in tension, $A_s F_y$. From equilibrium, the depth of the Whitney Stress Block, a, is calculated according to ACI 318-08 10.2.7.1 as

$$a = \frac{A_s F_y}{0.85 f_c' b_{eff}} \tag{3.4}$$

From this stress block, the location of the compressive force in the concrete is known to be $\frac{a}{2}$ from the top of the concrete slab.

Taking the moment about any reference point gives the nominal moment strength, $M_n$, of the composite beam. If the referent point is chosen at the interface,

$$M_n = T_s\left(\frac{d}{2}\right) + C_c\left(t_s - \frac{a}{2}\right) \tag{3.5}$$

where,

$T_s$ = full plastic capacity of the steel = $A_s F_y$

If the section is controlled by the concrete crushing, $V_c' < V_s'$, and the plastic neutral axis is in the steel. The concrete reaches its full capacity with

$$C_c = 0.85 f_c' b_{eff} t_s \tag{3.6}$$

The compressive and tensile forces in the steel need to be determined. To determine these forces, the location of the plastic neutral axis needs to be obtained. To do this, it first needs to be determined whether the plastic neutral axis is in the top flange of the steel, or in the web. If the plastic neutral axis is in the top flange

$$T_w + T_f = T_s - T_f < C_c \tag{3.7}$$

where, $T_w$ is the maximum tension in the web, and $T_f$ is the maximum tension in one flange. These values are determined by multiplying the respective areas of the steel by the yield strength, $F_y$. If the above statement is not true, the location of the plastic neutral axis is in the web of the steel beam.

To find the location of the neutral axis, an analysis of forces in the steel and concrete is performed. Considering the case where the neutral axis is in the top flange of the steel, the tensile force in the steel is expressed as

$$T = T_s - (b_f\, x) F_y \tag{3.8}$$

where,

$b_f$ = Steel flange width

$x$ = distance from the top of the steel flange to the location of the PNA

The total compressive force equals the sum of the compression in the concrete and the compression in the steel and is written as

$$C = C_c + (b_f\ x)F_y \tag{3.9}$$

The tensile and compressive forces can be set equal due to equilibrium. By doing this, the location of the plastic neutral axis in the top flange of the steel is given by

$$x = \frac{A_s F_y - C_c}{2\ b_f F_y} \tag{3.10}$$

At this point, all of the forces in the concrete and steel can be calculated. By taking the moment about a reference point, the nominal moment strength, $M_n$, of the composite beam is calculated. Choosing the reference point to be at the interface, the nominal moment strength of the composite beam can be expressed as

$$M_n = T_s\left(\frac{d}{2}\right) + C_c\left(t_s - \frac{a}{2}\right) - 2\ (b_f F_y x)\left(\frac{x}{2}\right) \tag{3.11}$$

### 3.3 Partial Interaction

When the maximum compressive and tensile force is controlled by the shear strength of the shear connection, a composite beam will experience what is called partial interaction. This means that the failure of the connection will cause the beam to fail before either the steel or concrete reach their limit states. When the studs limit the composite action, the shear force at the interface is written as

$$V_q' = \sum Q_n \tag{3.12}$$

where,

$Q_n$ = The shear strength of each shear stud

The shear strength of an individual stud is calculated using the equation given by AISC I8.2a which is

$$Q_n = 0.5A_{sa}\sqrt{f_c' E_c} \leq R_g R_p A_{sa} F_u \tag{3.13}$$

where,

$A_{sa}$ = cross-sectional area of the shear stud

$E_c$ = modulus of elasticity of concrete

$F_u$ = minimum tensile strength of the shear stud

$R_g$ = coefficient to account for group effect determined using to AISC I8.2a

$R_p$ = position effect factor for shear studs determined using to AISC I8.2a

$R_g$ and $R_p$ depend on the geometry and orientation of the steel decking and the configuration of the shear studs. In the case of a solid slab with a single row of shear studs, $R_g$ and $R_p$ equal 1.0 and 0.75 respectively. The left side of the inequality is an empirical equation that accounts for the limit state of the concrete crushing around the stud. The right side is an equation for the ultimate strength of the shear stud. Values of $Q_n$ are tabulated in AISC Table 3-21 for common situations.

To find the moment capacity of a partially composite beam, the same method for determining the strength of a fully composite beam with the PNA in the steel is used. The only difference here is that the concrete slab does not reach its full compressive strength. It is limited by the strength of the connection. When only partial interaction will occur, the value of the compressive force in the concrete slab is equal to the maximum shear force at the

interface, $V_q'$. If the PNA falls in the top flange of the steel beam, the calculation of the moment strength can be performed using equations 3.10 and 3.11 with $V_q'$ equal to $C_c$.

### 3.4 Analysis of Beam Tested

The beams tested had the geometry and loading configuration shown in Figure 3-2 and Figure 3-3. The beams contained 24 shear studs, 12 on each side of the midspan. An example of the calculation of the nominal moment strength of one of the beams tested is shown below. Data set 2 is used for the example. The test data sets can be seen in Table 3-1 and Figure 3-4 at the end of this chapter. The following calculation is based on AISC Chapter I, which has been previously outlined.

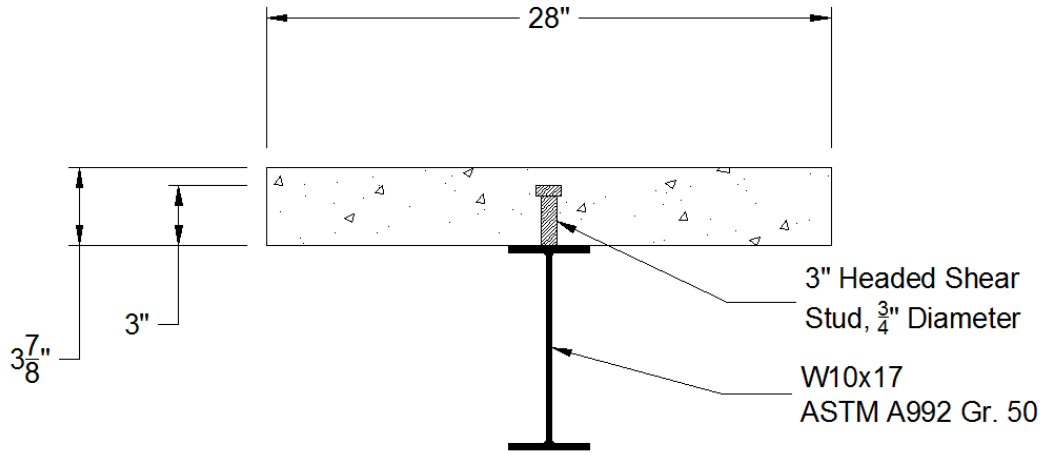


Figure 3-2 Cross Section of Test Beam

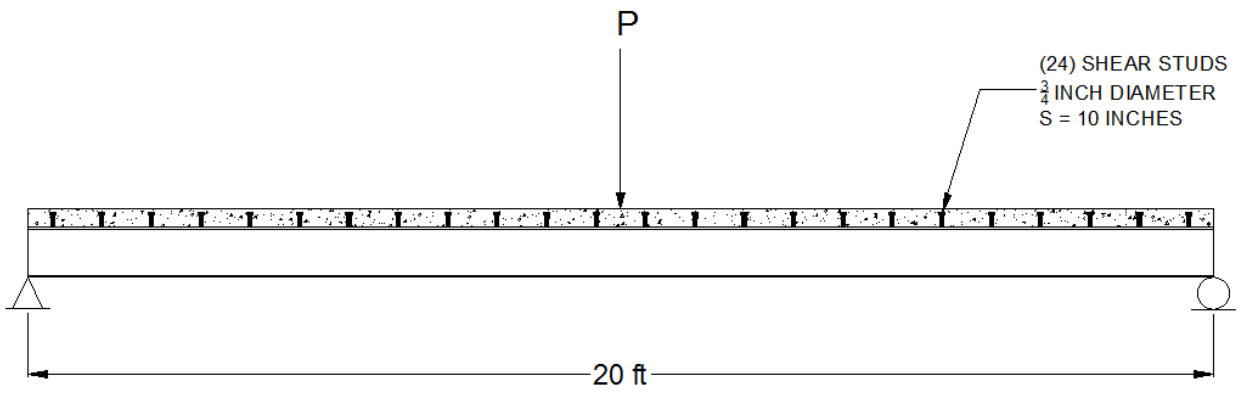


Figure 3-3 Composite Beam Lab Test Configuration

The effective width of the concrete slab which will provide composite action is the sum of the effective widths for each side. Due to symmetry, each side will have the same effective width, which is the lesser of:

1. 1/8 of the beam span = (20ft)(1/8) = 2.5 ft = 30 in
2. 1/2 of the beam spacing (not applicable)
3. Distance to the edge of the concrete slab = 14 in

The sum of the least effective widths for each side gives the total effective concrete slab width.

$$b_{eff} = (14\ in) + (14\ in) = 28 \text{ in}$$

To predict the strength of the composite beam, it must be determined whether the mode of failure is crushing of the concrete, yielding of the steel, or shear failure of the studs by comparing the shear forces at the interface for each of the given limit states.

$$\mathrm{V_c'} = 0.85 f_c' b_{eff} t_s = (0.85)(4000psi)(28in)\left(3\tfrac{7}{8}\,in\right)$$

$$= 368900\ lbs = \ 368.9\ \text{kips}$$

$$V_s' = A_s F_y = (4.99\ in^2)(50\ ksi) = 249.5\ kips$$

$$V_q' = \ \sum Q_n = 12\ (21.5\ kips) = 258\ kips$$

The value of $Q_n$ is obtained from AISC for a composite beam with a solid concrete slab with a compressive strength of 4,000 psi.

From here it is seen that the yielding of the steel will control the behavior since $V_c' > V_s'$ and $V_q' > V_s'$. This means that the composite beam is assumed to have full interaction between the concrete and steel. It also tells that the PNA will be located in the concrete section and the compressive force in the concrete, $C_c$, is equal to $A_s F_y$. To calculate the moment strength of the composite section, the location of $C_c$ needs to be determined. First the depth of the stress block is calculated.

$$a = \frac{A_s F_y}{0.85 f_c' b_{eff}} = \frac{249.5\ kips}{0.85(4\ ksi)(28\ in)} = 2.62\ inches$$

At this point, the nominal moment capacity of the composite beam can be calculated using equation (3.5).

$$M_n = T_s \left(\frac{d}{2}\right) + C_c \left(t_s - \frac{a}{2}\right)$$

$$M_n = \ (249.5\ kips\ ) \left(\frac{10.1\ in}{2}\right) + (249.5\ kips)(3\tfrac{7}{8}\ in - \ \frac{2.62\ in}{2})$$

$$M_n = \ 1900\ kip - in = 158.3\ \ kip - ft$$

To compare this strength value to the results of the beam tests, the concentrated load at midspan corresponding to this moment strength is needed. For a simply supported beam with a given concentrated load at the midspan, the moment at the midspan can be written as

$$M = \frac{PL}{4} \tag{3.14}$$

where,

P = concentrated load at midspan

L = span length of the beam

Having calculated the moment strength, the theoretical maximum concentrated load the beam can hold, $P_u$, can be calculated.

$$P_u = \frac{4M_n}{L} = \frac{4(158.3\ kip - ft)}{20\ ft} = 31.66\ kips$$

For the example provided, the actual concentrated load at midspan experienced during testing which caused the beam to fail was equal to 30 kips. The percent error of the estimation calculated per AISC is +5.53%. For the complete set of data the error in the estimations ranged from -0.30% to +19.2% with an average of a 6.6% overestimation.

Although the shear studs provide more than enough strength for the assumed distribution of forces in the concrete, neither the steel beams, nor the concrete slabs reach their full capacity. This tells us that the composite beams have not been experiencing full composite action as assumed. The stress distributions must be similar to what is shown in Figure 3-1. To analyze the degree of composite action experienced, the theory of partial

interaction can be used. From equation 3.11, the moment strength of a partially composite section with the PNA in the top flange of the steel is

$$M_n = T_s\left(\frac{d}{2}\right) + C_c\left(t_s - \frac{a}{2}\right) - 2\,(b_f F_y x)\left(\frac{x}{2}\right)$$

Since the total shear strength of the shear studs is calculated to be more than sufficient, $C_c$ becomes an unknown variable of interest. This equation can be rearranged by making several substitutions, and $C_c$ can be calculated. The substitutions are as follows:

(1) $M_n = \frac{PL}{4}$ using $P_u$ from the beam test results.

(2) $x = \frac{A_s F_y - C_c}{2\, b_f F_y}$ from equation 3.10

(3) $a = \frac{C_c}{0.85 f_c' b_{eff}}$ using the Whitney Stress Block

These substitutions yield the following expression:

$$-C_c^2\left(\frac{1}{2\left(0.85 f_c' b_{eff}\right)} + \frac{1}{4F_y b_f}\right) + C_c\left(t_s + \frac{A_s}{2b_f}\right) + \left(A_s F_y \frac{d}{2} - \frac{A_s^2 F_y}{4b_f} - \frac{PL}{4}\right) = 0 \qquad (3.15)$$

This expression is valid when the PNA is in the top flange of the steel, or when

$$0 \le x = \frac{A_s F_y - C_c}{2\, b_f F_y} \le t_f,$$

where $t_f$ is the thickness of the top flange of the steel. For the example provided, the actual $C_c$ that was experienced is calculated to be 188.9 kips using equation 3.15. Equation 3.15 is shown to be valid in this case since

$$0 \le x = \frac{A_s F_y - C_c}{2\, b_f F_y} = 0.151\ in\ \le t_f = 0.330\ in.$$

Knowing the value of x, the tensile force at failure can be calculated.

$$\mathrm{T} = T_s - (b_f\, x)F_y = \ 249.5\ kips - (4.01in)(0.151in)(50ksi) = \ 219.2\ kips$$

This shows that only 86.2% of the tensile force in the steel was transferred to the concrete at the time of failure. The values for each test data set have been calculated and are shown in Table 3-1. Of the ten sets of data, the amount of tension transferred from the steel to the concrete ranged from 64.4% to two cases of 100%. The average was 86.8%.

Load versus deflection graphs are also shown for the data. Figure 3-4 shows a compilation of all data sets. Figures 3-5 show the data compared to the methods suggested by Girhammar et al. and AISC. For the AISC load vs. deflection, a lower bound moment of inertia is used. The lower bound moment of inertia is a theoretical minimum moment of inertia including only the portion of concrete within the stress block at the point of full plastic behavior (Geschwindner 2008). The values for the lower bound moment of inertia are tabulated in AISC Table 3-20. These values were used for the plots shown in Figures 3-5. This lower bound moment of inertia is considered a conservative estimate since more concrete is likely contributing to the actual moment of inertia than at the time of failure. However, it is seen on the graphs that this estimate is not completely accurate. For many of the data sets, it is shown using the lower bound moment of inertia gives a fair indicator of the actual deflection. For data set 1, data set 2, and data set 3 the elastic deflections experienced were greater than the deflections predicted using the lower bound moment calculated by AISC.

In Figures 3-5, the deflections are also compared to the methods presented by Girhammar et al. (2009), which were discussed in Chapter 2. This method uses an effective

bending stiffness which accounts for partial interaction. This involves estimating the slip stiffness, K. For a non-composite section, the slip stiffness would be zero. A larger the slip stiffness is used for a higher degree of interaction. This parameter was left for the reader to estimate. The slip stiffness is difficult to estimate since the slip is small and the concrete properties are nonlinear. It was determined that using a slip stiffness of 9 ksi for every data set provided an accurate or conservative estimate, as seen in Figures 3-5. While this method has potential for easy implementation, a reliable method for predicting the slip stiffness needs to be determined.

## Test Data and Analysis

| | Data Set 1 12/5/2003 | | | Data Set 2 11/3/2004 | | | Data Set 3 3/30/2005 | |
|---|---|---|---|---|---|---|---|---|
| | f'c (psi)= | 4177 | | f'c (psi)= | 4000 | | f'c (psi)= | 5050 |
| | **LOAD (kips)** | **DEFLECTION (in)** | | **LOAD (kips)** | **DEFLECTION (in)** | | **LOAD (kips)** | **DEFLECTION (in)** |
| | 0.0 | 0 | | 0.0 | 0 | | 3.5 | 0.124 |
| | 8.0 | 0.538 | | 6.0 | 0.387 | | 4.6 | 0.169 |
| | 12.0 | 0.732 | | 8.0 | 0.469 | | 5.5 | 0.202 |
| | 16.0 | 0.969 | | 10.0 | 0.606 | | 6.9 | 0.261 |
| | 20.0 | 1.265 | | 12.0 | 0.68 | | 7.5 | 0.285 |
| | 22.0 | 1.507 | | 14.0 | 0.765 | | 10.0 | 0.391 |
| | 24.0 | 1.782 | | 16.0 | 0.859 | | 12.0 | 0.476 |
| | 26.0 | 2.155 | | 18.0 | 0.98 | | 13.9 | 0.555 |
| | 28.0 | 2.713 | | 20.0 | 1.19 | | 16.1 | 0.651 |
| | 30.0 | 4.5625 | | 22.0 | 1.372 | | 18.0 | 0.737 |
| | | | | 24.0 | 1.547 | | 20.2 | 0.837 |
| | | | | 26.0 | 1.889 | | 22.0 | 0.945 |
| | | | | 28.0 | 2.276 | | 23.9 | 1.087 |
| | | | | 30.0 | 3.593 | | 24.6 | 1.176 |
| | | | | 29.0 | 5.75 | | 25.8 | 1.289 |
| | | | | 28.0 | 7.75 | | 27.1 | 1.406 |
| | | | | 27.0 | 8.875 | | 28.1 | 1.557 |
| | | | | 0.0 | 7 | | 29.0 | 1.751 |
| | | | | | | | 30.0 | 1.964 |
| | | | | | | | 31.0 | 2.275 |
| | | | | | | | 32.0 | 2.733 |
| | | | | | | | 32.9 | 4.098 |
| | | | | | | | 29.0 | 6.033 |
| | | | | | | | | |

| | | | |
|---|---|---|---|
| **Max Load (kips)** | 30 | 30 | 32.9 |
| **AISC Nominal Load (kips)** | 31.89 | 31.66 | 32.8 |
| **% Error** | 6.30 | 5.53 | -0.30 |
| **Actual $C_c$ (kips)** | 185.2 | 188.9 | 249.5 |
| **Actual a (in)** | 1.86 | 1.98 | 2.08 |
| **Actual x (in)** | 0.160 | 0.151 | |
| **Actual T (kips)** | 217.42 | 219.22 | 249.50 |
| **% Tension Transferred** | 85.18 | 86.17 | 100.00 |

Table 3-1.1 Test Data and Analysis

| Test Data and Analysis | | | | | | | | |
|---|---|---|---|---|---|---|---|---|
| | **Data Set 4** 11/22/2005 | | | **Data Set 5** | | | **Data Set 6** 11/7/2007 | |
| | f'c (psi)= | 5050 | | f'c (psi)= | 4700 | | f'c (psi)= | 4200 |
| | **LOAD (kips)** | **DEFLECTION (in)** | | **LOAD (kips)** | **DEFLECTION (in)** | | **LOAD (kips)** | **DEFLECTION (in)** |
| | 0.0 | 0.002 | | 0.0 | 0 | | 3.4 | 0.118 |
| | 5.0 | 0.222 | | 5.0 | 0.165 | | 5.1 | 0.202 |
| | 7.0 | 0.301 | | 7.0 | 0.24 | | 7.1 | 0.298 |
| | 9.0 | 0.388 | | 9.0 | 0.334 | | 9.2 | 0.403 |
| | 11.0 | 0.472 | | 11.0 | 0.431 | | 11.2 | 0.501 |
| | 13.0 | 0.572 | | 13.0 | 0.525 | | 13.0 | 0.594 |
| | 15.0 | 0.667 | | 15.0 | 0.622 | | 15.2 | 0.709 |
| | 17.0 | 0.774 | | 17.0 | 0.716 | | 17.1 | 0.804 |
| | 19.0 | 0.908 | | 19.0 | 0.84 | | 19.2 | 0.914 |
| | 21.0 | 1.066 | | 21.0 | 1.021 | | 21.0 | 1.019 |
| | 23.0 | 1.261 | | 23.0 | 1.253 | | 23.0 | 1.133 |
| | 25.0 | 1.534 | | 25.0 | 1.528 | | 25.0 | 1.279 |
| | 28.0 | 2.143 | | 27.0 | 2.053 | | 27.0 | 1.493 |
| | 28.0 | 2.507 | | 27.3 | 5.1 | | 29.0 | 1.798 |
| | 29.0 | 3.9 | | 0.0 | 3.98 | | 31.0 | 2.265 |
| | 29.0 | 4.33 | | | | | 30.0 | 3 |
| | 27.2 | 6.77 | | | | | 30.0 | 4 |
| | 26.6 | 8.03 | | | | | 30.0 | 5 |
| | | | | | | | 30.0 | 6 |
| | | | | | | | | |
| | | | | | | | | |
| | | | | | | | | |
| | | | | | | | | |
| | | | | | | | | |
| | | | | | | | | |
| | | | | | | | | |
| **Max Load (kips)** | 29 | | | 27.25 | | | 31 | |
| **AISC Nominal Load (kips)** | 32.8 | | | 32.48 | | | 31.92 | |
| **% Error** | 13.10 | | | 19.19 | | | 2.97 | |
| **Actual $C_c$ (kips)** | 151.6 | | | 118.5 | | | 214.8 | |
| **Actual a (in)** | 1.26 | | | 1.06 | | | 2.15 | |
| **Actual x (in)** | 0.244 | | | 0.327 | | | 0.087 | |
| **Actual T (kips)** | 200.58 | | | 183.94 | | | 232.06 | |
| **% Tension Transferred** | 75.58 | | | 64.42 | | | 92.56 | |

Table 3-1.2 Test Data and Analysis

| Test Data and Analysis | | | | | | | |
|---|---|---|---|---|---|---|---|
| | Data Set 7 4/2/2008 | | | | | Data Set 8 10/26/2010 | |
| | f'c (psi)= | 5300 | | | | f'c (psi)= | 5173 |
| | **LOAD (kips)** | **DEFLECTION (in)** | **LOAD (kips)** | **DEFLECTION (in)** | | **LOAD (kips)** | **DEFLECTION (in)** |
| | 0.0 | 0 | 22.0 | 0.967 | | 0.0 | 0 |
| | 1.5 | 0.045 | 23.0 | 1.037 | | 3.1 | 0.109 |
| | 2.2 | 0.076 | 24.0 | 1.101 | | 6.0 | 0.257 |
| | 3.0 | 0.104 | 25.1 | 1.181 | | 9.2 | 0.427 |
| | 3.5 | 0.125 | 26.0 | 1.268 | | 12.0 | 0.561 |
| | 4.0 | 0.146 | 27.1 | 1.376 | | 15.1 | 0.713 |
| | 4.6 | 0.171 | 28.1 | 1.491 | | 18.0 | 0.86 |
| | 5.0 | 0.186 | 29.0 | 1.638 | | 21.2 | 1.082 |
| | 6.0 | 0.238 | 30.0 | 1.798 | | 24.0 | 1.373 |
| | 7.0 | 0.28 | 31.0 | 2.006 | | 27.0 | 1.875 |
| | 8.0 | 0.328 | 32.0 | 2.315 | | 29.8 | 4.25 |
| | 9.3 | 0.385 | 33.0 | 2.894 | | 0.0 | 3.67 |
| | 10.0 | 0.414 | 30.0 | 5.816 | | | |
| | 11.1 | 0.462 | 0.0 | 4.478 | | | |
| | 12.0 | 0.513 | | | | | |
| | 13.0 | 0.554 | | | | | |
| | 14.0 | 0.6 | | | | | |
| | 15.0 | 0.647 | | | | | |
| | 16.0 | 0.689 | | | | | |
| | 17.0 | 0.735 | | | | | |
| | 18.2 | 0.788 | | | | | |
| | 19.1 | 0.832 | | | | | |
| | 20.0 | 0.873 | | | | | |
| | 21.0 | 0.916 | | | | | |
| | | | | | | | |
| **Max Load (kips)** | 33 | | | | | 29.77 | |
| **AISC Nominal Load (kips)** | 33 | | | | | 32.9 | |
| **% Error** | 0.00 | | | | | 10.51 | |
| **Actual $C_c$ (kips)** | 249.5 | | | | | 167.3 | |
| **Actual a (in)** | 1.98 | | | | | 1.36 | |
| **Actual x (in)** | 0.00 | | | | | 0.205 | |
| **Actual T (kips)** | 249.50 | | | | | 208.40 | |
| **% Tension Transferred** | 100.00 | | | | | 80.28 | |

Table 3-1.3 Test Data and Analysis

| Test Data and Analysis | | | | | |
|---|---|---|---|---|---|
| | **Data Set 9** 3/22/2011 | | | **Data Set 10** 10/28/2011 | |
| | f'c (psi)= | 5700 | | f'c (psi)= | 3042 |
| | **LOAD (kips)** | **DEFLECTION (in)** | | **LOAD (kips)** | **DEFLECTION (in)** |
| | 0.0 | 0 | | 0.0 | 0 |
| | 5.1 | 0.195 | | 2.1 | 0.017 |
| | 10.0 | 0.418 | | 3.7 | 0.075 |
| | 15.1 | 0.664 | | 5.8 | 0.171 |
| | 19.9 | 0.931 | | 8.0 | 0.282 |
| | 25.0 | 1.417 | | 10.1 | 0.372 |
| | 30.0 | 2.368 | | 12.0 | 0.469 |
| | 30.8 | 3.5 | | 14.1 | 0.566 |
| | 29.4 | 5.017 | | 15.8 | 0.661 |
| | 0.0 | 3.704 | | 18.0 | 0.771 |
| | | | | 20.0 | 0.884 |
| | | | | 22.0 | 1.022 |
| | | | | 24.3 | 1.225 |
| | | | | 26.0 | 1.5 |
| | | | | 28.0 | 2.3 |
| | | | | 29.3 | 3.41 |
| | | | | 29.9 | 5.5 |
| | | | | 0.0 | 4.169 |
| | | | | | |
| | | | | | |
| | | | | | |
| | | | | | |
| | | | | | |
| | | | | | |
| | | | | | |
| **Max Load (kips)** | 30.8 | | | 29.88 | |
| **AISC Nominal Load (kips)** | 33.29 | | | 29.95 | |
| **Percent Error** | 8.08 | | | 0.23 | |
| **Actual $C_c$ (kips)** | 185.9 | | | 241.3 | |
| **Actual a (in)** | 1.37 | | | 3.33 | |
| **Actual x (in)** | 0.159 | | | 0.020 | |
| **Actual T (kips)** | 217.62 | | | 245.49 | |
| **% of Tension Transferred** | 85.42 | | | 98.29 | |

Table 3-1.4 Test Data and Analysis

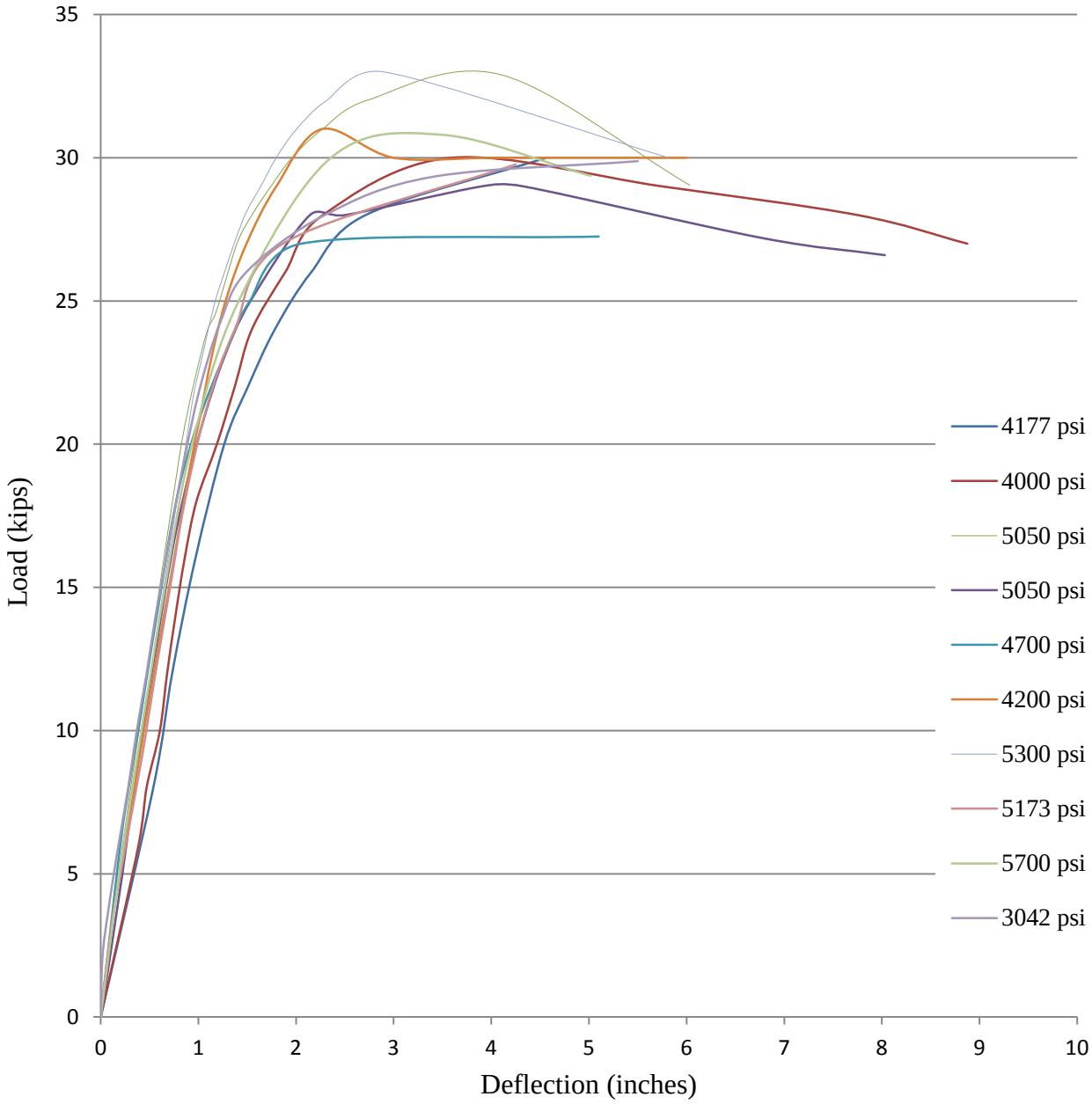


Figure 3-4 Load vs. Deflection for all Data Sets

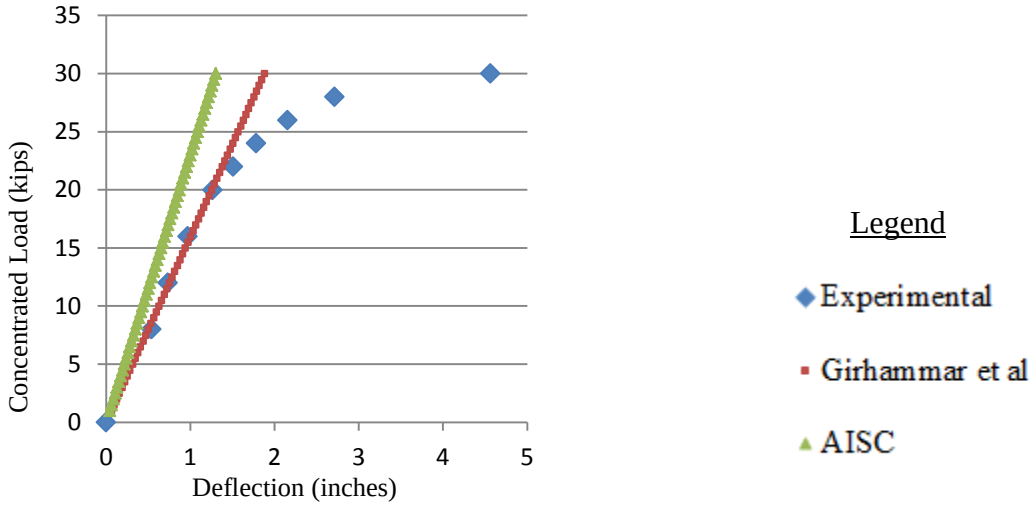


Figure 3-5.1 Load vs. Deflection Data Set 1

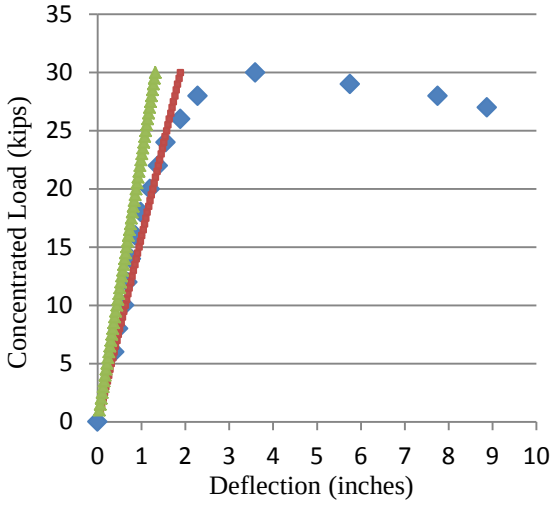


Figure 3-5.2 Load vs. Deflection Data Set 2

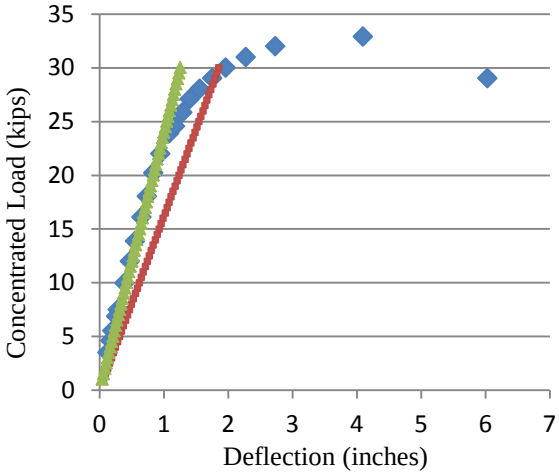


Figure 3-5.3 Load vs. Deflection Data Set 3

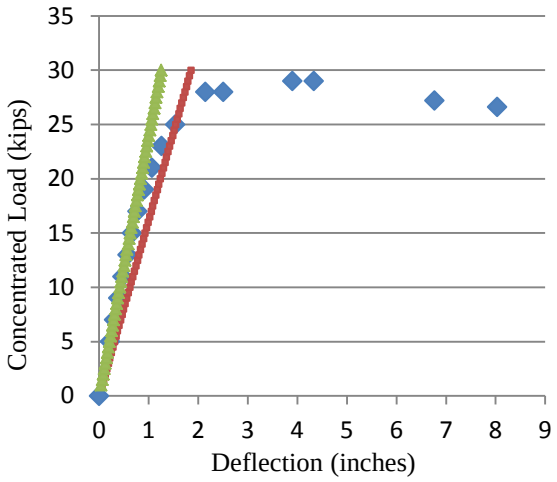


Figure 3-5.4 Load vs. Deflection Data Set 4

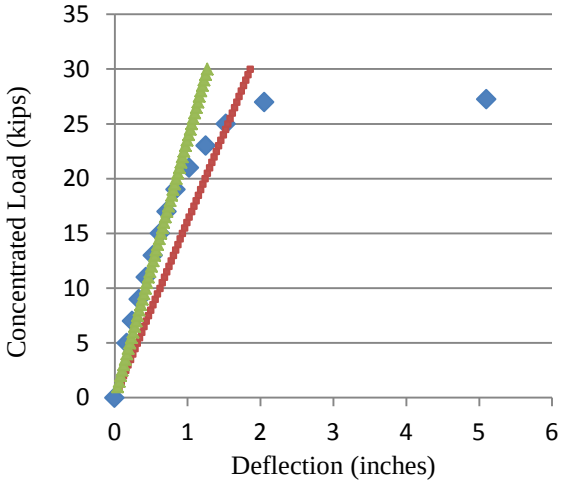


Figure 3-5.5 Load vs. Deflection Data Set 5

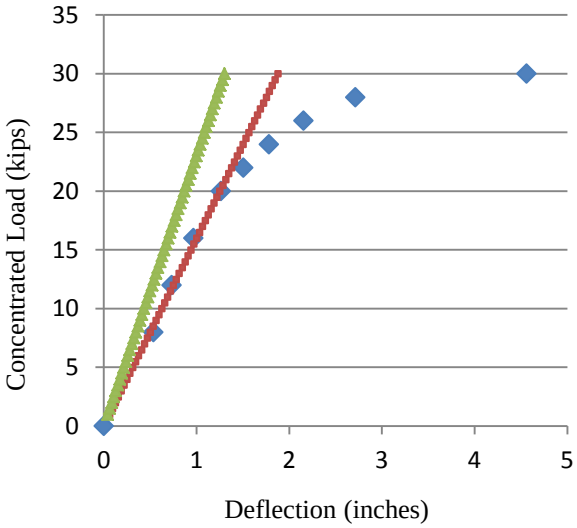


Figure 3-5.6 Load vs. Deflection Data Set 6

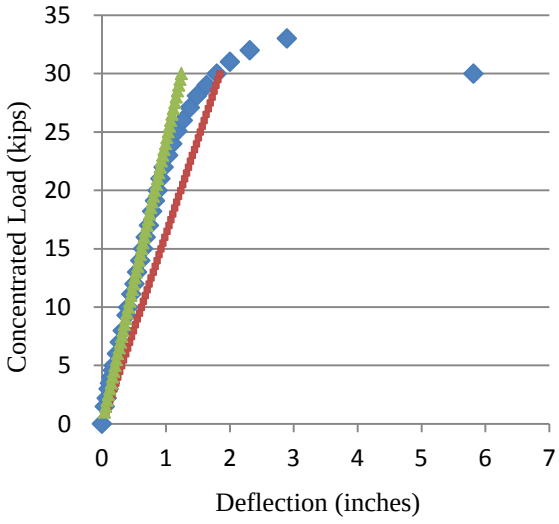


Figure 3-5.7 Load vs. Deflection Data Set 7

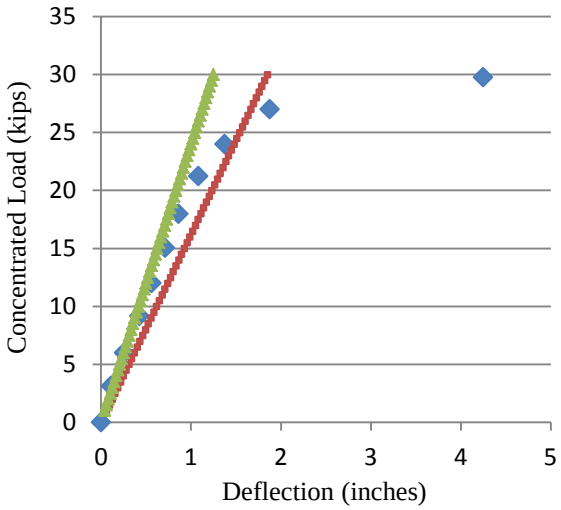


Figure 3-5.8 Load vs. Deflection Data Set 8

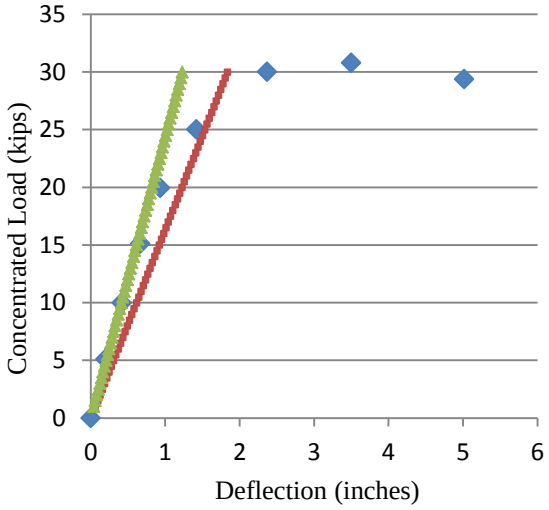


Figure 3-5.9 Load vs. Deflection Data Set 9

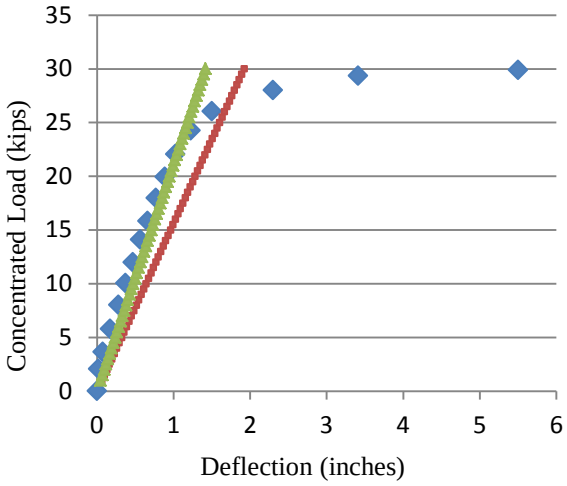


Figure 3-5.10 Load vs. Deflection Data Set 10

# Chapter 4 Finite Element Model

## 4.1 General

Using SAP2000, the composite beam was modeled. The model consisted of area elements for the slab, and frame elements for the beam and studs. The elements were given the same geometries and properties as the materials of beams tested to allow for direct comparison. The model was analyzed in both the elastic and plastic range. The beam was simply supported with a concentrated load at midspan. Figure 4-1 shows a conceptual view of the finite element model. A detailed description of the model formation and analysis is given in the following sections of this chapter.

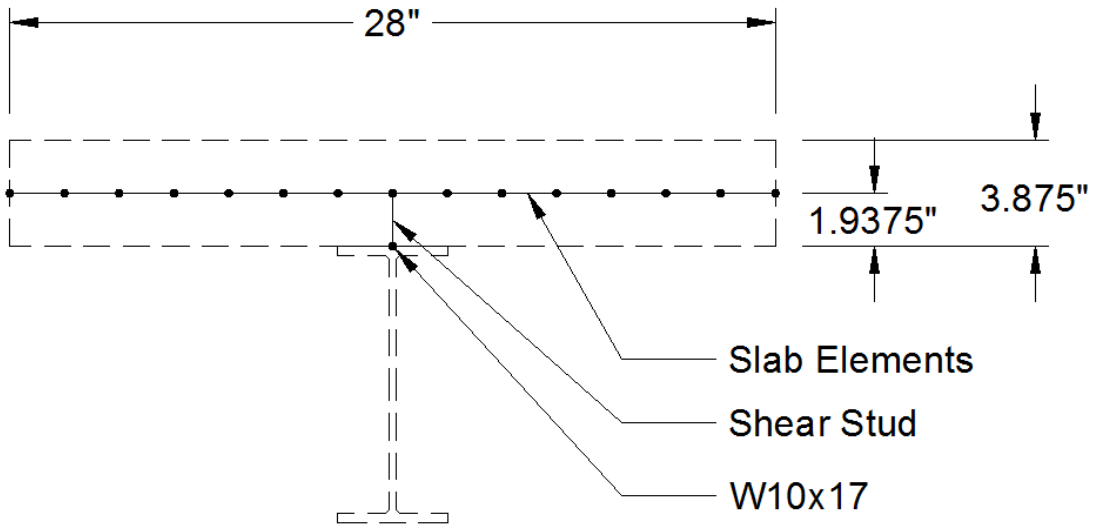


Figure 4-1 Conceptual View of Finite Element Model

**4.2 Elements**

Each component of the composite beam was modeled using elements with defined geometries and properties to match the beam tested. The steel beam was modeled using a two node frame element. The frame element material was given the properties of ASTM A992 Grade 50 steel. Additionally, the section properties for a W10x17 shape beam were imported and assigned to the frame. The frame element has six degrees of freedom and is capable of carrying both axial force and moment.

Although the properties of ASTM A992 Grade 50 steel have been assigned to the frame elements, SAP2000 will not automatically recognize the point at which the section begins to experience nonlinear behavior. To allow for nonlinear analysis of the steel beam, hinges must be assigned at discrete locations along the beam. A hinge is defined to allow strength loss in a section when the yield stress is reached. In the composite section, both axial force and moment are present in the beam. To prevent the beam from exceeding its capacity, hinges have been assigned every inch along the beam. At the hinges, the internal forces in the steel section are checked against the combined axial force and flexure interaction equations H1-1a and H1-1b given by AISC. If the section has yielded, the strength is reduced and the forces from that section are redistributed. After the strength is reduced, the steel section undergoes strain hardening.

The concrete slab is modeled using shell elements formed from areas. The areas are 2 inches by 1 inch, and the shell is given a thickness of $3^{7}/_{8}$ inches. A series of these shell elements is used to represent the entire slab. To do this, four node area elements are given concrete properties and a thickness to represent the slab. The concrete used for the model is

typical 4000 psi compressive strength concrete. Areas are often used to carry either in-plane shear forces or bending moments only. The shell element is capable of carrying both.

To model the shear studs, frame elements are also used. This element is assigned the cross section of the shear stud and the properties of ASTM A108 steel, which is the standard headed shear stud material. For the shear studs, a length equal to half the thickness of the concrete slab is used. Although this length, $1^{7}/_{16}$ inches, is less than the actual length of the shear stud, the shear area remains the same. The slab section is connected to the top of the stud, which allows for the concrete to be flush with the top of the steel beam since the concrete shell sections will be extruded in both directions.

The basis of the model was made using these three elements. A ten inch section of this concept is shown in Figure 4-2 below. The extruded view of the elements in this section is shown in Figure 4-3.

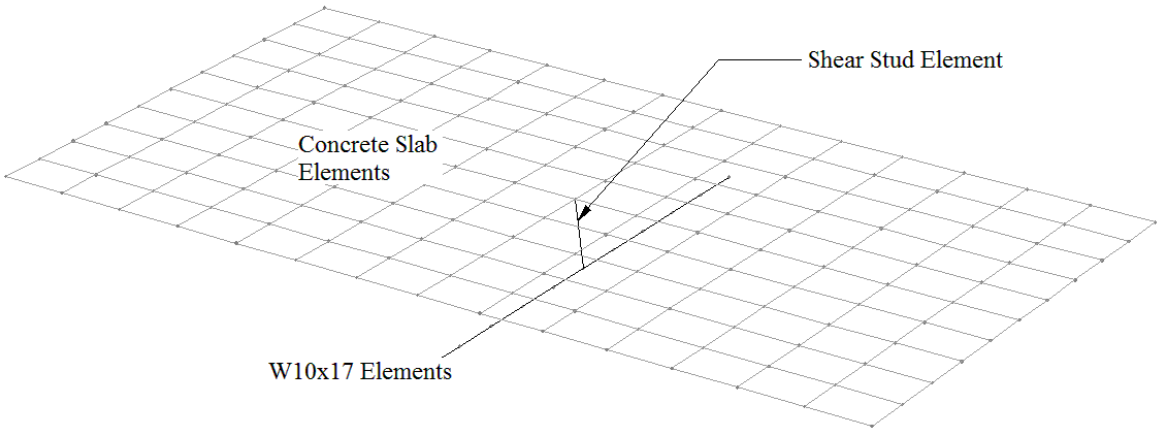


Figure 4-2 Basic Elements

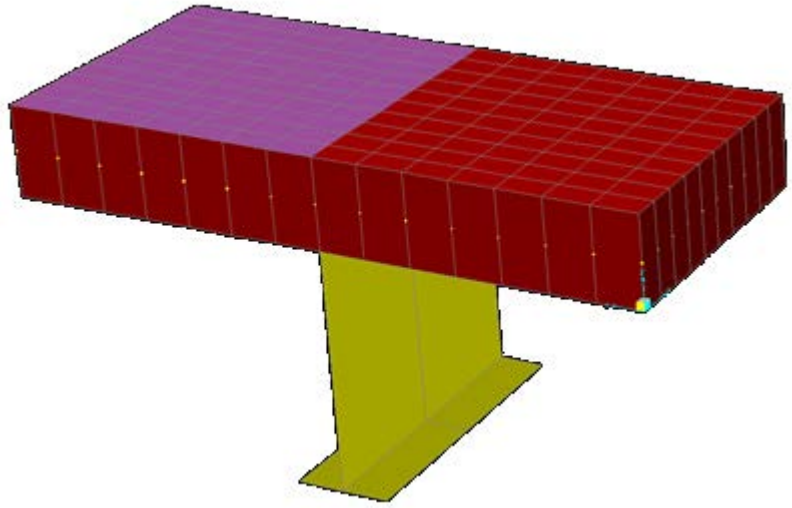

Figure 4-3 Extruded View of Basic Elements

This basic section was repeated 23 times to model the entire 20 foot beam. Adjacent sections share common nodes, allowing the sections to act as one continuous beam.

**4.3 Supports and Connectivity**

The composite beam is supported by pin and roller supports connected to the steel beam elements and not the slab. This is done to match the configuration in the lab setting. Although the supports in the lab likely provide some constraint at the ends, it is conservative to assume that both ends can rotate freely.

With the basic arrangement, the concrete slab is only supported by the shear studs. Leaving the studs to support the concrete alone would cause unrealistic behavior and shear force distributions in the concrete. In reality, the concrete beam is continuously supported in the vertical direction by the steel beam. To model this support, frame elements were used discretely at 1 inch increments along the beam. To allow these supporting elements to support the frame in the vertical direction without absorbing shear forces, the moment of

inertia for these elements was set to zero. Additionally, the ends of the support elements were released so they could not transfer any moment. With these modifications to the supporting element properties, the elements can provide support to the slab in the vertical direction while letting shear forces pass through. The elements supporting the concrete slab between the shear studs are shown Figure 4-4. A gap between the nodes of elements is used to represent the released ends of the supports. To add stability to the slab, restraints were also added to the four corners of the slab to prevent rotation about the longitudinal axis of the composite beam.

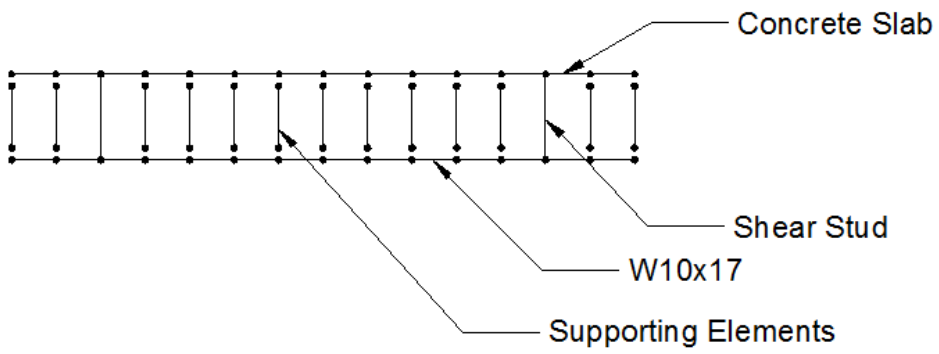


Figure 4-4 Concrete Supporting Elements

Adding slab supports at one inch increments requires the concrete slab and steel beam elements to be a maximum of one inch long. Using one inch elements is also beneficial for obtaining more refined results.

**4.4 Loading**

The model was loaded with a concentrated load at midspan. To evaluate the beam under elastic behavior, incremental loads were assigned. These incremental loads allow the evaluation of the composite beam behavior during elastic behavior including deflections, and

internal forces and moments. For these loads, linear static cases were used. By evaluating the linear static cases, the elastic limit is determined in Chapter 5.

Once the elastic limit is exceeded, the linear static load cases no longer provide valid results. After this point, it is necessary to use nonlinear static load cases to utilize the previously described hinges in the analysis. Only material nonlinearities were considered in the load cases. Geometric nonlinearities were ignored.

# Chapter 5 Results and Analysis

## 5.1 Elastic Behavior

At first, linear static load cases were run on the model. The results show both moment and axial force in the steel and concrete. To determine the load at the point where the steel begins to yield, the stress in the extreme tension fiber must be calculated. Since the stress in each material is caused by both axial force and moment, both must be considered in the calculation. In this case, the stress in the extreme tension fiber, $f_t$, can be calculated using the equation

$$f_t = Mc/I + P/A \tag{5.1}$$

where,

$M$ = the moment in the steel beam

$c$ = the distance from the centroid to the extreme tension fiber

$P$ = the axial force in the steel beam

$A$= the cross-sectional area of the steel

When the stress in the extreme tension fiber reaches the yield stress of steel, 50 ksi, the elastic limit has been reached. As seen in Table 5-1, the plastic limit occurs when the concentrated load is about 21.25 kips. A visual inspection of the load versus displacement graphs of the test data can give an indication of the load at which the elastic limit was reached during the lab tests. This will be the load corresponding with the approximate location on the graph where the deflection no longer increases linearly. From Figure 3-4, the

elastic limit seems to have been reached under a concentrated load between 20 kips and 25 kips. Table 5-1 gives a summary of the behavior of the model in the elastic range. These values can be compared to the test data in Figure 5-1. Table 5-2 shows a comparison between the SAP2000 model and the lower bound stiffness calculated in accordance with AISC.

| **Results for composite beam with simple supports** | | | | | |
|---|---|---|---|---|---|
| **Load** | **Axial Force** | **Moment** | **$f_T$** | **Deflection** | **$EI_x$** |
| Kips | Kips | Kip-in | ksi | Inches | ksi-in$^4$ |
| 1 | 4.30 | 24.2 | 2.36 | 0.045 | 6407404 |
| 5 | 21.48 | 121.2 | 11.78 | 0.225 | 6407404 |
| 10 | 42.96 | 242.4 | 23.56 | 0.449 | 6407390 |
| 15 | 64.44 | 363.6 | 35.33 | 0.674 | 6407395 |
| 20 | 85.93 | 484.8 | 47.11 | 0.899 | 6407390 |
| 21 | 90.22 | 509.0 | 49.47 | 0.944 | 6407391 |
| 21.25 | 91.30 | 515.1 | 50.06 | 0.955 | 6407391 |

Table 5-1 Model Output within the Elastic Range

| **Elastic deflections for design in accordance with AISC** | | | | | |
|---|---|---|---|---|---|
| **Load** | **E** | **I** | **$EI_x$ AISC** | **Deflection** | **% Diff in EI with model** |
| Kips | ksi | in$^4$ | ksi-in$^4$ | inches | |
| 1 | 29000 | 226.6 | 6571400 | 0.044 | -2.53 |
| 5 | 29000 | 226.6 | 6571400 | 0.219 | -2.53 |
| 10 | 29000 | 226.6 | 6571400 | 0.438 | -2.53 |
| 15 | 29000 | 226.6 | 6571400 | 0.657 | -2.53 |
| 20 | 29000 | 226.6 | 6571400 | 0.877 | -2.53 |
| 21 | 29000 | 226.6 | 6571400 | 0.920 | -2.53 |
| 21.25 | 29000 | 226.6 | 6571400 | 0.931 | -2.53 |

Table 5-2 AISC Calculations for Model

As shown in Tables 5-1 and 5-2, the lower bound stiffness method given by AISC overestimates the stiffness of the model with a percent difference of 2.53. The lower bound stiffness also underestimated the deflection of the test beams stiffness as discussed in Chapter

3 and shown in Figures 3-5. The actual stiffness of a composite section is affected by the degree of interaction occurring between the steel beam and concrete slab. The analysis in Chapter 3 shows that full interaction, which is assumed for the lower bound moment of inertia calculation, is not actually achieved. The occurrence of partial composite action causes less of the concrete to act in compression, which would decrease the lower bound moment of inertia.

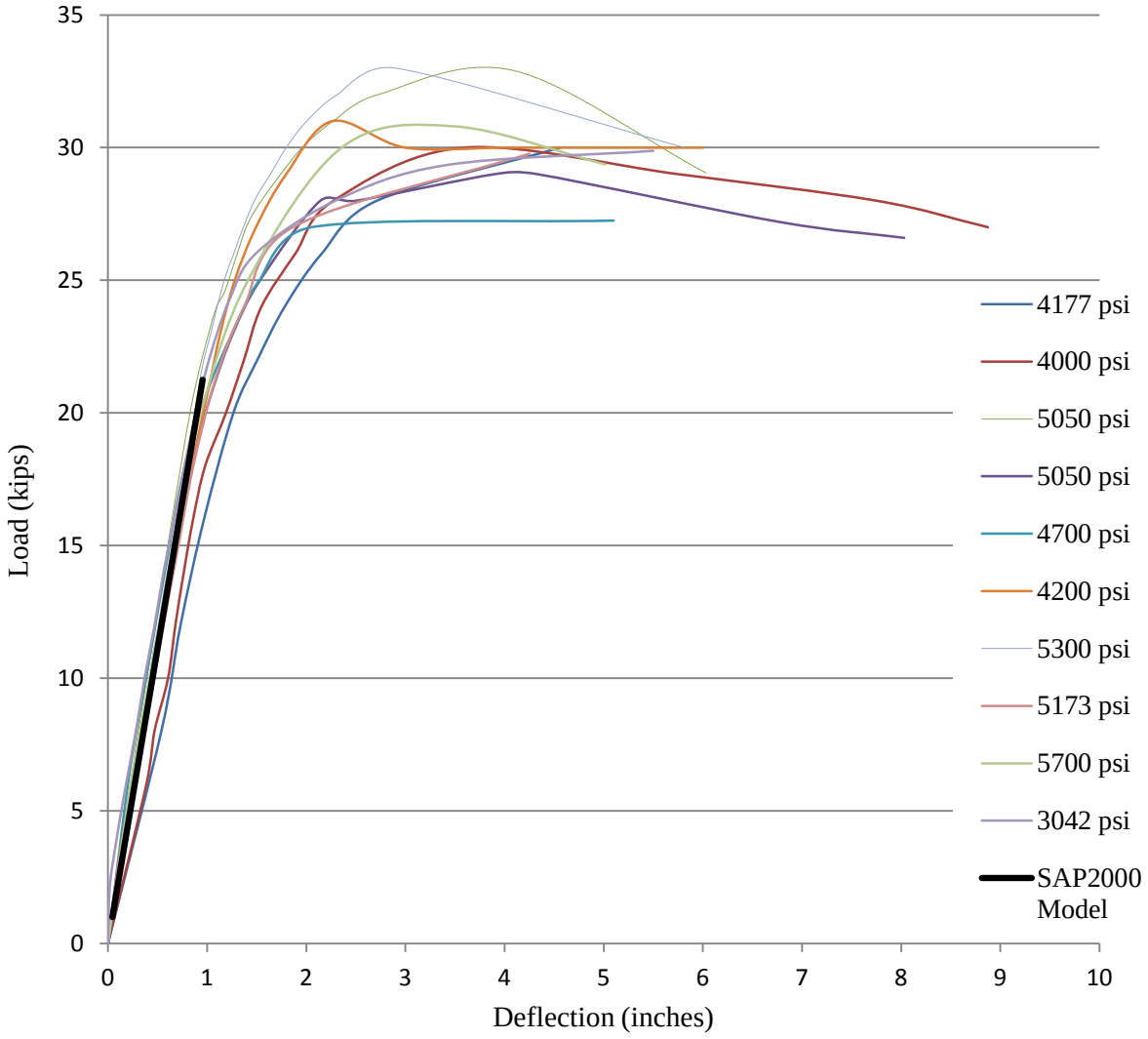


Figure 5-1 Comparison of Elastic Deflections to Test Data

The elastic deflections of the model used are compared to the test data. The model provides a slightly more accurate prediction load-deflection behavior than AISC, but is still not conservative. This is caused by the nonlinear properties of concrete, and the analysis capabilities of SAP2000. Although a portion of the concrete slab would develop cracks and would not contribute to bending stiffness, this is not accounted for in the analysis.

SAP2000 does not have the capability to properly analyze the behavior of the concrete slab. Concrete is extremely nonlinear. According to the American Concrete Institute, the tensile strength of concrete is variable, and typically ranges from 10% to 15% of the compressive strength. Concrete will not develop large tensile forces. When a moment is experienced, the concrete will hold the forces in compression, but not tension. This causes the need for the tension to be carried by the steel beam.

This nonlinearity is not used in the analysis of shell elements by SAP2000. During analysis, SAP2000 will properly model the regions of concrete that are in compression. However, the regions in tension caused by internal moments will sustain more load than concrete is actually capable of holding. Instead of transferring most of the compressive forces to the steel to be carried in tension, the shell elements allow for large internal moments to be resisted in the concrete. This causes smaller axial forces and higher moment in the steel beam, which in turn cause smaller transverse shear forces at the interface.

The nonlinear analysis provided by SAP2000 allows yielding of the steel beam. The analysis shows that the steel beam has reached yield, and entered the strain hardening stage when the nominal load predicted by AISC is reached. While this is the behavior that is expected, it is calculated using larger moments and smaller axial forces than actually

experienced. The true value in this analysis comes from the distribution of longitudinal forces in the concrete slab.

### 5.2 Slab Force Distributions

The stress distribution in the concrete slab is assumed to be uniform by AISC. The distribution of forces across the concrete slab produced with the model output can be seen in Figure 5-1. The distribution of forces shown occurred during the nonlinear analysis of the composite beam under the nominal concentrated load predicted by AISC, 31.66 kips. In Figure 5-2 the top of the image is the midspan location on the composite beam. The distribution of forces is shown using the color scale given on the side of the image. The compressive forces in the slab increase toward the center of the slab near the shear studs. A concentration of compressive forces is formed around the studs. The stress concentration is especially apparent toward the end of the steel beam. The end studs experience this stress concentration because the shear forces need to be transferred even though the slab is not in as much compression as it is at midspan. The stress distributions near the end studs are shown in an enlarged view in Figure 5-3

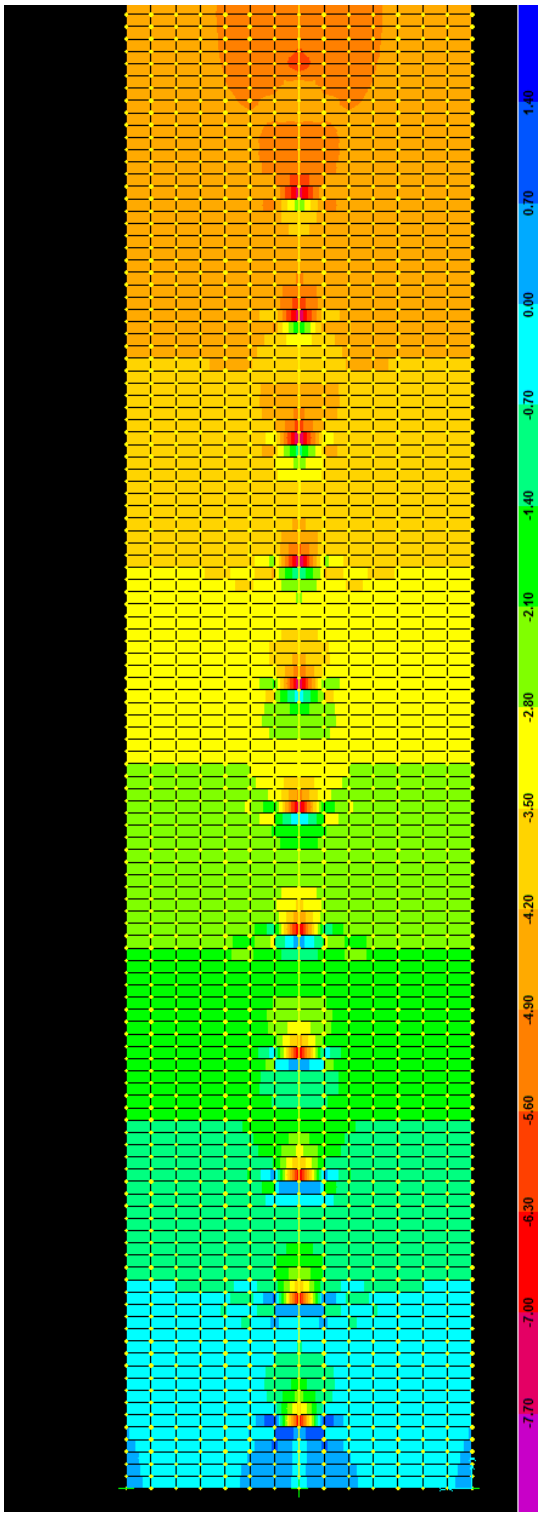


Figure 5-2 Concrete Slab Force Distribution

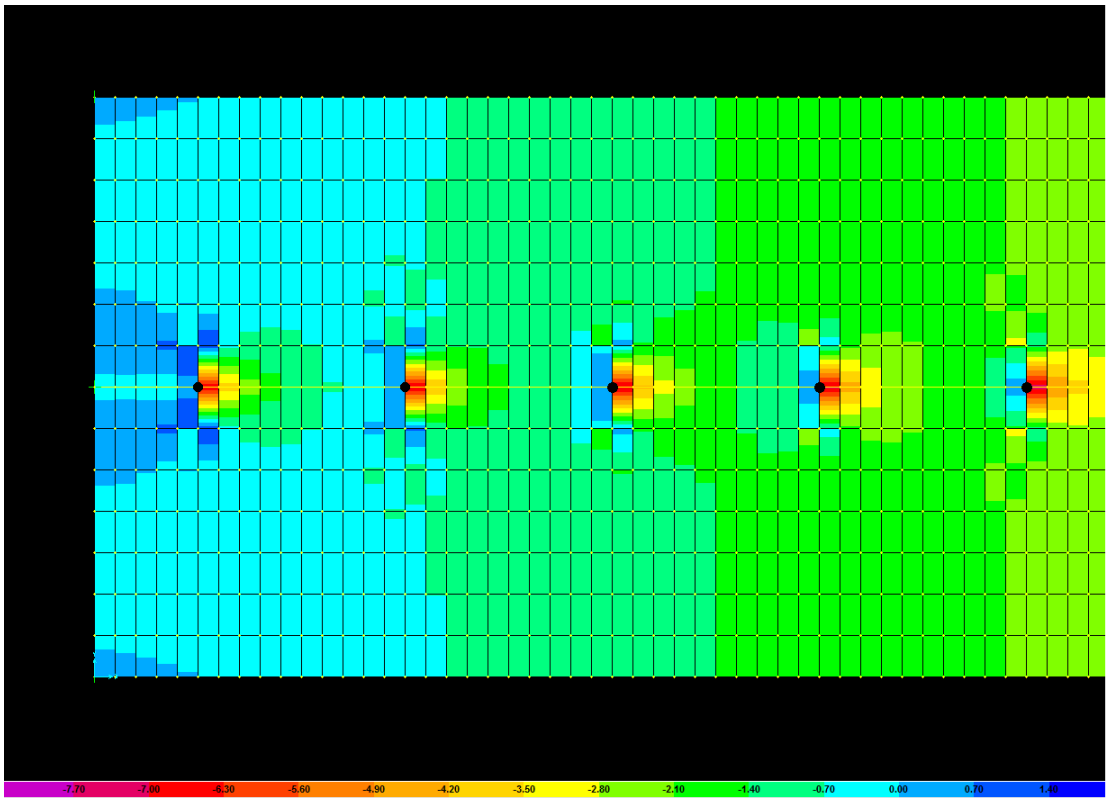


Figure 5-3 Enlarged View of Concrete Slab Force Distribution near End Studs

These concentrations are shown graphically in Figure 5-4. The stresses in the concrete just before a stud are increasingly concentrated further away from midspan of the composite beam. The force distributions at various studs are shown. The studs on each side of the midspan location are numbered 1 through 12 with 1 being the stud the stud closest to midspan and 12 being the end stud.

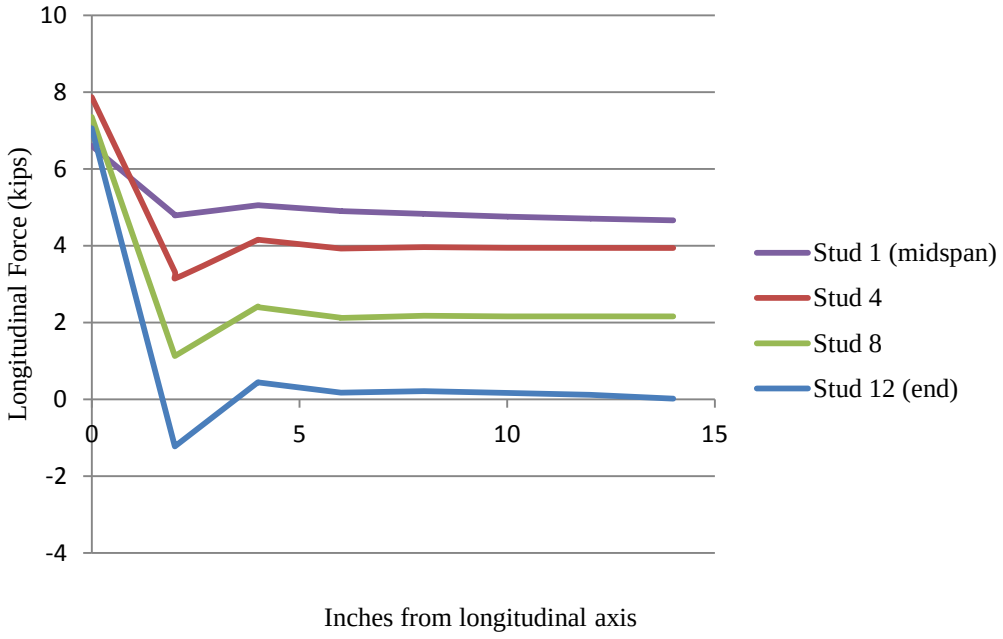


Figure 5-4 Force Distributions across Concrete Slab at 4 Stud Locations

The models show that the majority of the compressive forces in the slab are resisted over a width of about 2 to 3 inches across the slab. In addition to a force concentration near the studs, tensile forces tend to develop directly next to the end stud in the model. As discussed, tensile forces in concrete will cause cracking to occur.

This is consistent with observations made during lab tests. Longitudinal cracks often developed in the concrete slab. This typical crack is pictured in Chapter 1, Figure 1-3. For the beam tested in data set 10, the concrete was removed from the end studs, shown in Figure 5-5, to allow the studs to be observed. The deflection in each of the four end studs was measured to be about $^{1}/_{8}$ inch. Although the studs are not always perfectly vertical, the observation of 4 studs consistently deflected toward the end of the beam is an indication that end slip was allowed by the deflection of the shear studs. The relative movement of the slab

in relation to the steel beam was also measured using the method discussed in Chapter 1. This measurement was also approximately $^1/_8$ inch. While neither of these measuring methods provides precision, consistency across the methods suggests that an end slip of $^1/_8$ inch occurred. This not only confirms that only partial interaction occurs, but it also indicates that that studs are experiencing larger shear forces than predicted.

Figure 5-5 End Stud with Concrete Removed

After observation of the studs, a sledge hammer was used to gain a feel for the remaining strength of the studs. The studs were impacted with the sledge hammer using mostly the force of gravity from a height of a few feet. The studs were broken off rather easily. A deformed and broken stud is shown in Figure 5-6. Although this test is not valid for analytical purposes, it is certainly a strong indication that the studs experienced a significantly higher shear force than expected.

Figure 5-6 Shear Stud after Low Impact with Sledge Hammer

**5.3 Shear Forces in Headed Shear Studs**

Shear studs experiencing more shear than expected may be caused by an uneven distribution of shear on the studs along the beam. The shear forces in the studs on the beam in the model were examined. Table 5-3 shows the values of shear forces in the studs along the beam. The same numbering scheme is used for the studs as Figure 5-4. Four load values are shown. These loads are the load causing nominal moment strength prediction (31.66 kips), the load which yield was experienced in the model using the interaction equation method discussed in Chapter 4 (28 kips), the load at the elastic limit (21.25 kips), and a load in the elastic range (15 kips). Along with the shear forces in each stud, the total shear force, and the ratio to maximum shear force in a single stud to assumed constant shear value is calculated. The values of these shear forces are plotted in Figure 5-7.

| Shear Forces on Studs Along Beam with 10 in. spacing | | | | |
|---|---|---|---|---|
| **Stud** | **P= 31.66 kips** | **P=28 kips** | **P= 21.25 kips** | **P= 15 kips** |
| 1 | 4.44 | 2.80 | 1.69 | 1.19 |
| 2 | 8.09 | 5.93 | 4.19 | 2.96 |
| 3 | 9.88 | 8.10 | 5.92 | 4.18 |
| 4 | 11.12 | 9.58 | 7.12 | 5.03 |
| 5 | 11.97 | 10.60 | 7.95 | 5.61 |
| 6 | 12.57 | 11.30 | 8.51 | 6.01 |
| 7 | 12.98 | 11.78 | 8.90 | 6.28 |
| 8 | 13.27 | 12.12 | 9.17 | 6.47 |
| 9 | 13.46 | 12.35 | 9.34 | 6.60 |
| 10 | 13.56 | 12.48 | 9.46 | 6.68 |
| 11 | 13.64 | 12.56 | 9.52 | 6.72 |
| 12 | 13.67 | 12.59 | 9.52 | 6.72 |
| Total | 138.7 | 122.2 | 91.3 | 64.4 |
| Assumed: | 11.55 | 10.18 | 7.61 | 5.37 |
| $\frac{V(max)}{V(total)}$ | 0.099 | 0.103 | 0.104 | 0.104 |
| $\frac{V(max)}{V(assumed)}$ | 1.183 | 1.237 | 1.252 | 1.252 |

Table 5-3 Shear Forces in Studs along Composite Beam

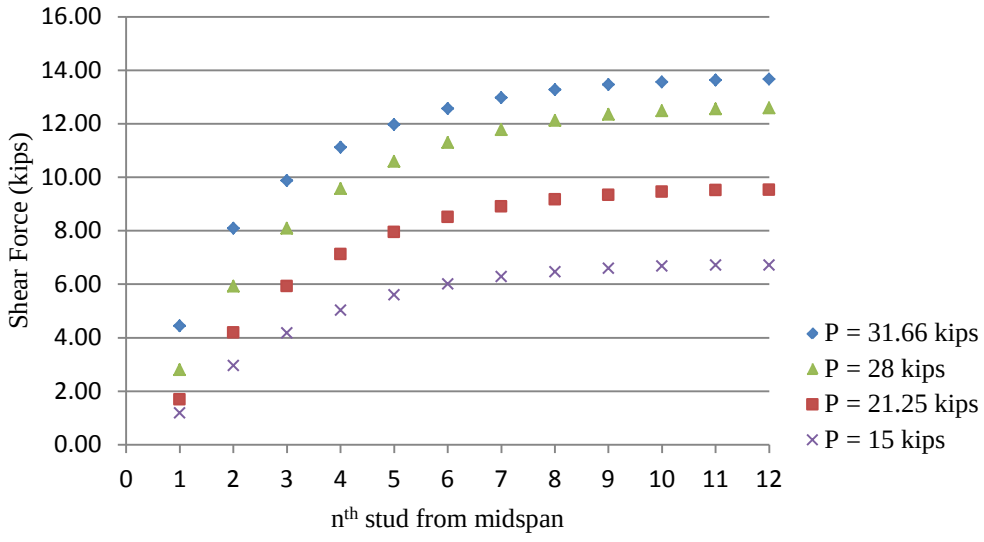


Figure 5-7 Shear Forces in Studs along Axis of Composite Beam

Within the elastic range, the ratio of maximum shear experienced to the assumed constant value is, V(max)/V(assumed), is constant. Once the steel beam has yielded, the shear forces in the studs deviate less from the predicted value. With this information, it is suggested by the model that the shear force in the stud may be as high as 1.25 times the predicted value. This is used to analyze the test data. Since the compressive strength of concrete used in the model is 4000 psi, data set two will again be used as an example.

The lesser of the total shear force, *V'*, calculated using equations 3.2, 3.3, and 3.12 is the expected total shear force.

$$V_c' = 0.85 f_c' b_{eff} t_s = (0.85)(4000psi)(28in)\left(3\tfrac{7}{8}\,in\right) = 368.9\ kips$$

$$V_s' = A_s F_y = (4.99\ in^2)(50\ ksi) = 249.5\ kips$$

$$V_q' = \sum Q_n = 12\ (21.5\ kips) = 258\ kips$$

From these calculations the total shear force, *V'*, is expected to be 249.5 kips. Using the methods of AISC, the force per stud is expected to be

$$\frac{V'}{n} = \frac{249.5\ kips}{12\ studs} = 20.8\ kips/stud$$

where n is the number of studs between $V_{max}$ and V = 0 determined from the shear diagram. Increasing this expected shear gives a value of

$$20.8 \frac{kips}{stud} * 1.25 = 26\ kips/stud$$

Revisiting equation 3.4 can place this in terms of shear connection strength.

$$Q_n = 0.5A_{sa}\sqrt{f_c' E_c} \leq R_g R_p A_{sa} F_u$$

$$Q_n = 0.5(\frac{\pi(0.75)^2}{4})\sqrt{(4)ksi\ (3492)ksi} \leq (1.0)(.75)\left(\frac{\pi(0.75)^2}{4}\right)65ksi$$

$$Q_n = 26.1\ kips \leq 21.5\ kips$$

Because the resulting shear force in the end stud may be as high as 26 kips, the studs may experience a shear force that is beyond their capacity. This excessive shear force may cause stud deflection, slip, and failure. Additionally, the shear force is only slightly below the value at which the concrete is expected to fail in this example. The observations made in the lab on the composite beams and the studs after being loaded are consistent with this analysis.

However, this calculation has only been shown to be relevant for the case of a steel, W10x17 beam joined to a 3 $^7/_8$ inch concrete slab with 24 headed shear studs. To evaluate the effect of slab thickness and width on the distribution, two more models were run. The existing model was modified to create one version with a different effective width and one with a different thickness. Since the effective slab width of 28 inches is less than typical, a model with a larger effective width was used. The $b_{eff}$ used for this model is the maximum allowable, taking $^1/_8$ span length on each side. The other modified version of the model was tested with a slab thickness of 2 ¾ inches. Since the V(max)/V(assumed) value is observed to decrease after the yield stress in the steel has been reached, the load corresponding to the elastic limit is used. These loads are calculated using equation 5.1. The results can be seen in table 5-4.

| | W10x17 Composite Beam | |
|---|---|---|
| | s = 10 in | s = 10 in |
| | $b_{eff}$ = 60 in | $b_{eff}$ = 28 in |
| | t= 3.875 in | t= 2.75 in |
| **Stud** | P = 23 kips | P = 19 kips |
| 1 | 1.71 | 2.19 |
| 2 | 4.22 | 4.99 |
| 3 | 5.99 | 6.63 |
| 4 | 7.26 | 7.60 |
| 5 | 8.17 | 8.16 |
| 6 | 8.82 | 8.50 |
| 7 | 9.28 | 8.69 |
| 8 | 9.61 | 8.81 |
| 9 | 9.84 | 8.88 |
| 10 | 9.98 | 8.93 |
| 11 | 10.07 | 8.93 |
| 12 | 10.09 | 8.86 |
| Total | 95.0 | 91.2 |
| Assumed: | 7.92 | 7.60 |
| $\frac{V(max)}{V(total)}$ | 0.106 | 0.098 |
| $\frac{V(max)}{V(assumed)}$ | 1.274 | 1.165 |

Table 5-4 Shear Distributions with Various Slab Dimensions

The tables show an increase in V(max)/V(assumed) with an increase in slab effective width. Also, a decrease is observed with a decrease in slab thickness. In the case of a large effective width, increasing the expected shear by 1.25 may not provide a conservative estimate. However, the V(max)/V(assumed) values for the models with effective widths equal to 60 inches and 28 inches are within 2% of each other. Also, this value is expected to decrease after the steel yields, therefore the difference in values is not a concern. For a slab thickness of 2.75 inches, the V(max)/V(assumed) value decreases, therefore expecting a shear of 1.25 times greater than predicted by AISC is still a conservative estimate.

To compare this method to other typical composite beams, two additional models were created. The models were given the same properties as the previous models. The models were again provided with a single row of shear studs, and loaded with a concentrated load at midspan. Both models were designed using the guidelines of AISC. The load causing the elastic limit to be reached was found using equation 5.1. The design details and shear distributions in the shear studs can be seen in Table 5-5.

The results show that these typical composite beams with concentrated loads at midspan also experience higher values of shear than assumed. These models experienced shear values that were 20.2% and 17.7% higher than expected respectively. From here, it is shown that typical models with larger dimensions and loads than the beam tested will have larger shear forces in the studs than predicted, but still with 25% of the assumed value.

| W18x35 Composite Beam | |
|---|---|
| | s = 8 in |
| | $b_{eff}$ = 64 in |
| | t= 3.875 in |
| | Span = 32 ft |
| **Stud** | **P= 41 kips** |
| 1 | 1.055 |
| 2 | 2.726 |
| 3 | 4.044 |
| 4 | 5.102 |
| 5 | 5.953 |
| 6 | 6.638 |
| 7 | 7.189 |
| 8 | 7.632 |
| 9 | 7.989 |
| 10 | 8.276 |
| 11 | 8.507 |
| 12 | 8.693 |
| 13 | 8.843 |
| 14 | 8.964 |
| 15 | 9.061 |
| 16 | 9.14 |
| 17 | 9.202 |
| 18 | 9.25 |
| 19 | 9.285 |
| 20 | 9.307 |
| 21 | 9.315 |
| 22 | 9.306 |
| 23 | 9.276 |
| 24 | 9.213 |
| Total | 184.0 |
| Assumed: | 7.665 |
| $\frac{V(max)}{V(total)}$ | 0.050 |
| $\frac{V(max)}{V(assumed)}$ | 1.202 |

| W14x26 Composite Beam | |
|---|---|
| | s = 10 in |
| | $b_{eff}$ = 80 in |
| | t= 3 in |
| | Span = 30ft |
| **Stud** | **P= 27.25 kips** |
| 1 | 1.773 |
| 2 | 4.26 |
| 3 | 5.965 |
| 4 | 7.157 |
| 5 | 7.994 |
| 6 | 8.586 |
| 7 | 9.006 |
| 8 | 9.305 |
| 9 | 9.519 |
| 10 | 9.673 |
| 11 | 9.784 |
| 12 | 9.863 |
| 13 | 9.917 |
| 14 | 9.949 |
| 15 | 9.957 |
| 16 | 9.936 |
| 17 | 9.875 |
| 18 | 9.744 |
| Total | 152.3 |
| Assumed: | 8.459 |
| $\frac{V(max)}{V(total)}$ | 0.064 |
| $\frac{V(max)}{V(assumed)}$ | 1.177 |

Table 5-5 Shear Distributions in Typical Composite Beams

# Chapter 6 Conclusion

## 6.1 Summary

It was observed in lab tests that composite beams with a single row of headed shear studs loaded with a concentrated load at midspan frequently fail before the nominal strength predicted by AISC is reached. Specific observations that were made include the presence of interlayer slip and the development of longitudinal cracking of the concrete slab. An analysis shows that these slabs do not actually achieve full interaction, although it is assumed for design.

Available literature has been reviewed to gain knowledge on the current understanding of the behavior of a composite beam. While some of the literature has shown to provide relatively accurate results, in general the methods are too complex and time consuming for design purposes.

A finite element model of the composite beam tested was developed to analyze the observed behavior and make design recommendations. The analyses show a concentration of forces in the concrete slab around the shear studs. Uneven distributions of the shear forces in the studs along the beam were also observed.

## 6.2 Conclusions

1. While AISC provides an empirical equation to determine the strength of a shear stud, uneven shear distribution in the studs is not considered. The models developed show that using a constant shear force is not accurate.
2. It is recommended that the uniform shear force that is currently used for design by AISC be increased by a factor of 1.25 to provide a conservative

design approach. This method of estimating the actual shear force that may be experienced by a shear stud is only valid for composite beams consisting of a steel, W shape and a solid concrete slab connected with a single row of headed shear studs subjected to a concentrated load at midspan.

## References

*AISC Steel Construction Manual* (2011). (14th ed.) American Institute of Steel Construction.

*Building Code Requirements for Structural Concrete (ACI 318-08) and Commentary* (2008). American Concrete Institute.

da Silva, A. R., & Sousa, J. B., J. (2009). A family of interface elements for the analysis of composite beams with interlayer slip. *Finite Elements in Analysis and Design, 45*(5), 305-314.

Fabbrocino, G., Manfredi, G., & Cosenza, E. (1999). Non-linear analysis of composite beams under positive bending. *Computers and Structures, 70*(1), 77-89.

Faella, C., Martinelli, E., & Nigro, E. (2002). Steel and concrete composite beams with flexible shear connection: "exact" analytical expression of the stiffness matrix and applications. *Computers and Structures, 80*(11), 1001-1009.

Gara, F., Leoni, G., & Dezi, L. (2009). A beam finite element including shear lag effect for the time-dependent analysis of steel-concrete composite decks. *Engineering Structures, 31*(8), 1888-1902.

Gara, F., Ranzi, G., & Leoni, G. (2010). Short-and long-term analytical solutions for composite beams with partial interaction and shear-lag effects. *International Journal of Steel Structures, 10*(4), 359-372.

Geschwindner, L. (2008). *Unified design of steel structures* (1st ed.). Hoboken, NJ: John Wiley & Sons, Inc.

Girhammar, U. A. (2009). A simplified analysis method for composite beams with interlayer slip. *International Journal of Mechanical Sciences, 51*(7), 515-30.

Girhammar, U. A., & Gopu, V. K. A. (1993). Composite beam-columns with interlayer slip - exact analysis. *Journal of Structural Engineering New York, N.Y., 119*(4), 1265-1282.

Girhammar, U. A., & Pan, D. H. (2007). Exact static analysis of partially composite beams and beam-columns. *International Journal of Mechanical Sciences, 49*(2), 239-255. doi:10.1016/j.ijmecsci.2006.07.005

Gupta, V. K., Okui, Y., Inaba, N., & Nagai, M. (2007). Effect of concrete crushing on flexural strength of steel-concrete composite girders. *Doboku Gakkai Ronbunshuu A, 63*(3), 475-485

He, S., Li, P., & Shang, F. (2011). Three dimensional simulation of steel-concrete composite beams with an interface-slip model. Paper presented at the *2011 International Conference on Structures and Building Materials, ICSBM 2011, January 7, 2011 - January 9, 163-167.* pp. 1520-1524.

Jurkiewiez, B. (2009). Static and cyclic behaviour of a steel-concrete composite beam with horizontal shear connections. *Journal of Constructional Steel Research, 65*(12), 2207-16.

Leon, R., Viest, I. (1997). Theories of incomplete interaction in composite beams. In Buckner, C., Shahrooz, B. (Ed.), *Composite construction in steel and concrete III* (pp. 858) American Society of Civil Engineers.

Liu, H., Liu, W., & Zhang, Y. (2005). Calculation analysis of shearing slip for steel-concrete composite beam under concentrated load. *Applied Mathematics and Mechanics (English Edition), 26*(6), 735-740.

Liu, Q. (2011). Ultimate load of composite beam based on effect for cracks in the brittle material on slip of shear connectors. Paper presented at the *2011 International Conference on Structures and Building Materials, ICSBM 2011, January 7, 2011 - January 9, 163-167.* pp. 1901-1904.

Mirza, O., & Uy, B. (2011). Effect of strain profiles on the behavior of shear connectors for composite steel-concrete beams. Paper presented at the *6th International Conference on Composite Construction in Steel and Concrete, July 20, 2008 - July 24,* pp. 160-172.

Naithani, K. C., & Gupta, V. K. (1988). Behaviour of a composite steel-beam-concrete-slab combination. *Indian Concrete Journal, 62*(10), 535-540.

Qureshi, J., Lam, D., & Ye, J. (2011). Effect of shear connector spacing and layout on the shear connector capacity in composite beams. *Journal of Constructional Steel Research, 67*(4), 706-19.

Ramm, W., Jenisch, F. (1996). Load-bearing behaviour of composite slabs as a part of composite beams. In Buckner, C., Shahrooz, B. (Ed.), *Composite construction in steel and concrete III* (pp. 673) American Society of Civil Engineers.

Ranzi, G., Bradford, M. A., & Uy, B. (2004). A direct stiffness analysis of a composite beam with partial interaction. *International Journal for Numerical Methods in Engineering, 61*(5), 657-672.

Ranzi, G., & Zona, A. (2007). A steel-concrete composite beam model with partial interaction including the shear deformability of the steel component. *Engineering Structures, 29*(11), 3026-3041.

Sapountzakis, E.J. & Katsikadelis, J.T. (2003). A new model for the analysis of composite steel - concrete slab and beam structures with deformable connection. *Mechanics, 31*, 340-349.

Segura, J. M. (1990). An approximate method of determination of shear stresses due to flexure in composite beams. *International Journal of Engineering Science, 28*(8), 735-50.

Spacone, E., & El-Tawil, S. (2004). Nonlinear analysis of steel-concrete composite structures: State of the art. *Journal of Structural Engineering, 130*(2), 159-168.

Xue, W., Ding, M., Wang, H., & Luo, Z. (2008). Static behavior and theoretical model of stud shear connectors. *Journal of Bridge Engineering, 13*(6), 623-634.

Yu-Fei Wu, & Xu, R. (2007). Two-dimensional analytical solutions of simply supported composite beams with interlayer slips. *International Journal of Solids and Structures, 44*(1), 165-75.

Zhao, G., & Li, A. (2008). Numerical study of a bonded steel and concrete composite beam. *Computers & Structures, 86*(19-20), 1830-8.

Zona, A., & Ranzi, G. (2011). Finite element models for nonlinear analysis of steel-concrete composite beams with partial interaction in combined bending and shear. *Finite Elements in Analysis and Design, 47*(2), 98-118.

# ACADEMIC VITA

**David C. Leaf**
dcl5076@psu.edu

3104 West Summit Ave
Downingtown, PA 19335

## EDUCATION:

**Bachelor of Science in Civil Engineering** (structures) anticipated May 2012
**Engineering Leadership Development Minor**
The Pennsylvania State University, University Park, Pennsylvania

## LEADERSHIP:

**Courses**

- Leadership Principles
- Leadership Innovation and Global Resource Challenges
- Global Engineering Teams
- International Leadership of Enterprise and Development

## EXPERIENCE:

**Civil Engineering Intern**
The Louis Berger Group, Exton, PA
May 2011 to August 2011

- Supported the Buildings & Facilities and Transportation divisions
- Developed components of designs and plans for bridge replacements, structural inspections, and general facilities
- Responsible for numerous calculations including quantity and cost estimations
- Organized and edited reports and contract documents for submittals and proposals

## HONORS AND ACTIVITIES:

Penn State Schreyer Honors College
American Society of Civil Engineers Student Chapter (member)
American Institute of Steel Construction (student member)
American Concrete Institute (student member)
Prestressed Concrete Institute (student member)
United States Naval Academy Leadership Conference
George M. Wildasin Memorial Trustee Scholarship recipient
Webber Roy Irvin Scholarship recipient
Frank Holzer Civil Engineering Scholarship recipient